

Electronic Supplementary Information

Allosteric Cooperativity in Ternary Complexes with Low Symmetry

Hongxin Chai, Liu-Pan Yang, Hua Ke, Xin-Yu Pang, and Wei Jiang*
*Department of Chemistry, Southern University of Science and Technology,
Xueyuan Blvd 1088, Shenzhen, 518055, P. R. China*
**E-mail: jiangw@sustc.edu.cn*

Table of Contents

1. Properties of 2a and 2b	S2
2. Characterization Data of Host-Guest Complexes	S7
3. Single Crystal X-Ray Crystallography	S33
4. Experimental Section	S35
4.1 General Method	S35
4.2 Synthetic Route of 2a and 2b	S35
4.3 Synthesis of guests D9D-2BArF and D10D-2BArF	S40
5. References	S45

1. Properties of 2a and 2b

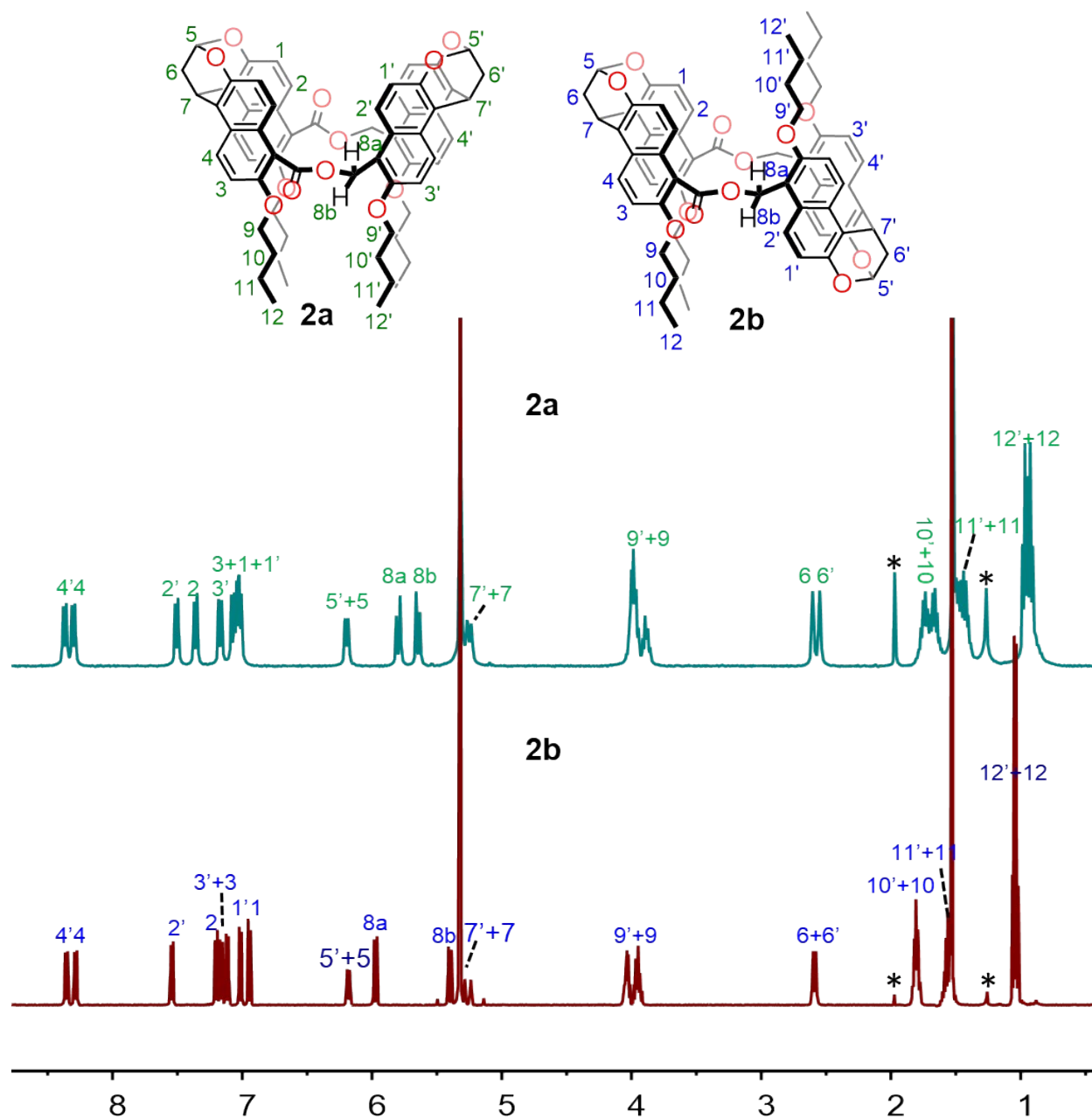


Fig. S1 Chemical structures and ¹H NMR spectra (500 MHz, CD₂Cl₂, 298 K) of two isomers of bis-ester naphthotubes **2a** (the one with high polarity) and **2b** (the one with low polarity). Peaks were assigned according to the following 2D NMR spectra. “*” indicates solvent impurities.

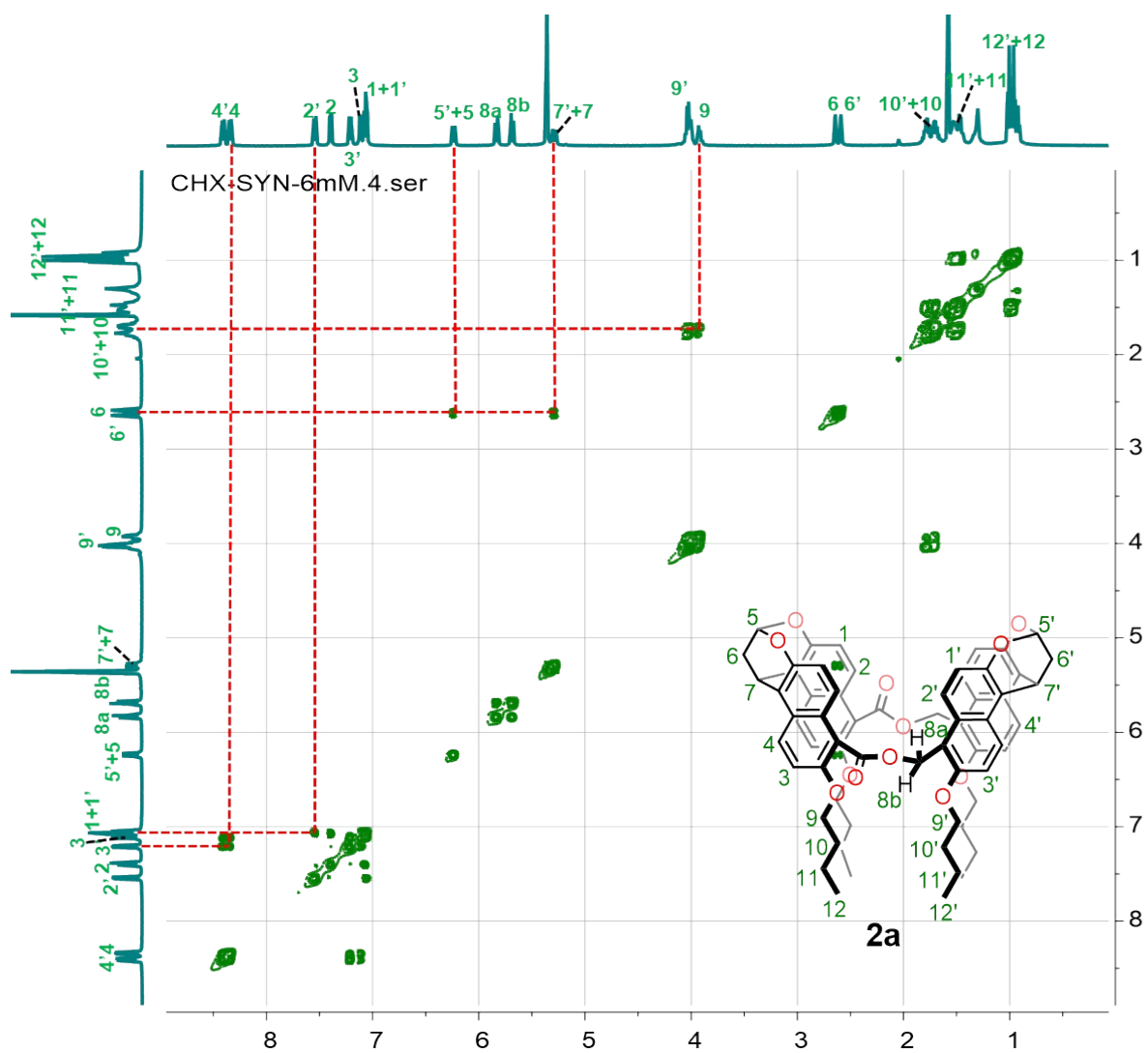


Fig. S2 $^1\text{H}, ^1\text{H}$ -COSY NMR spectrum (500 MHz, CD_2Cl_2 , 298 K) of **2a**.

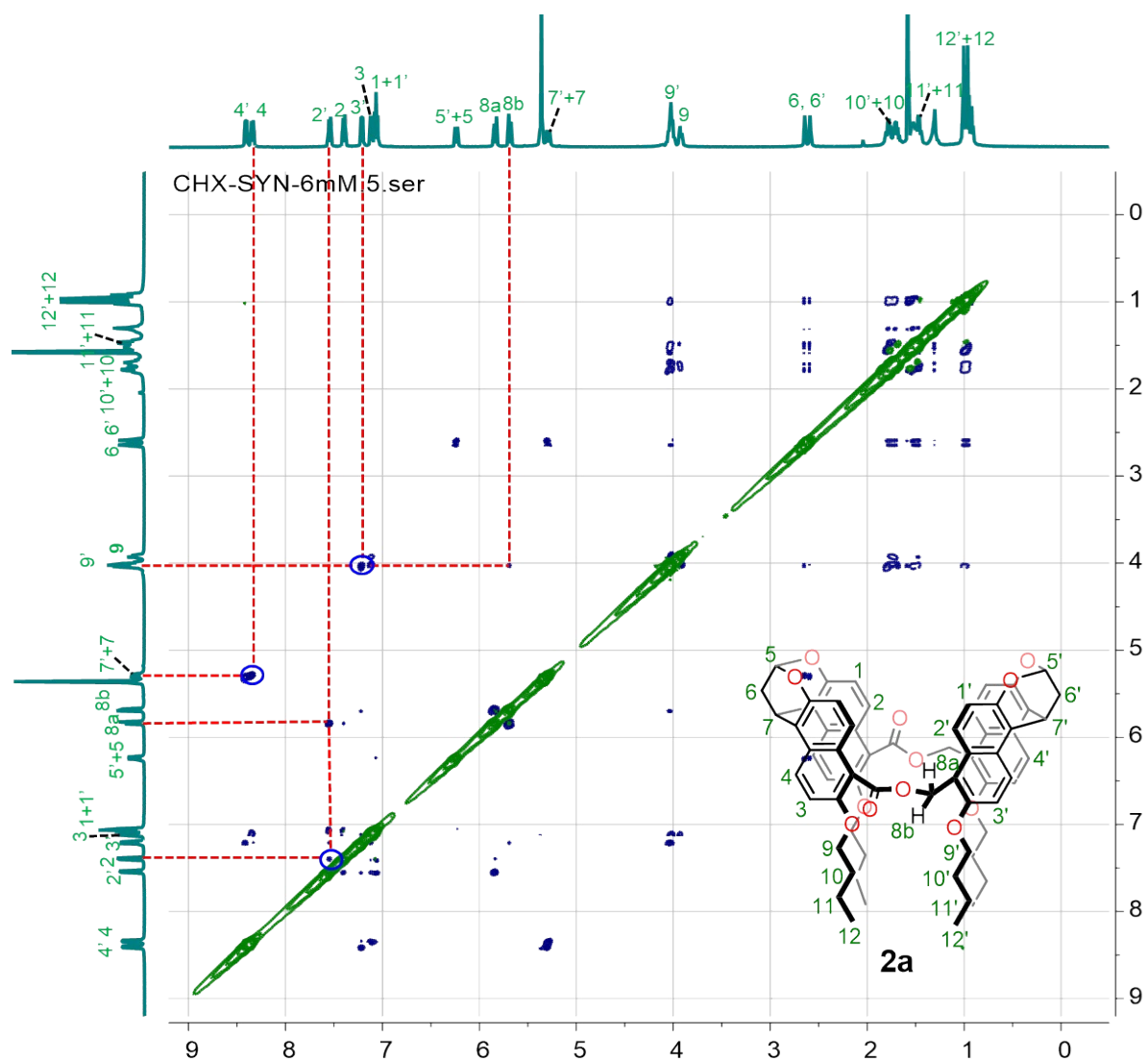


Fig. S3 $^1\text{H},^1\text{H}$ -ROESY NMR spectrum (500 MHz, CD_2Cl_2 , 298 K) of **2a**. No NOE effect was detected between the alkyl protons (9-12) and aromatic protons (1 and 2). But NOE contact between protons 2 and 2' was observed, which suggests this isomer as the *syn* compound.

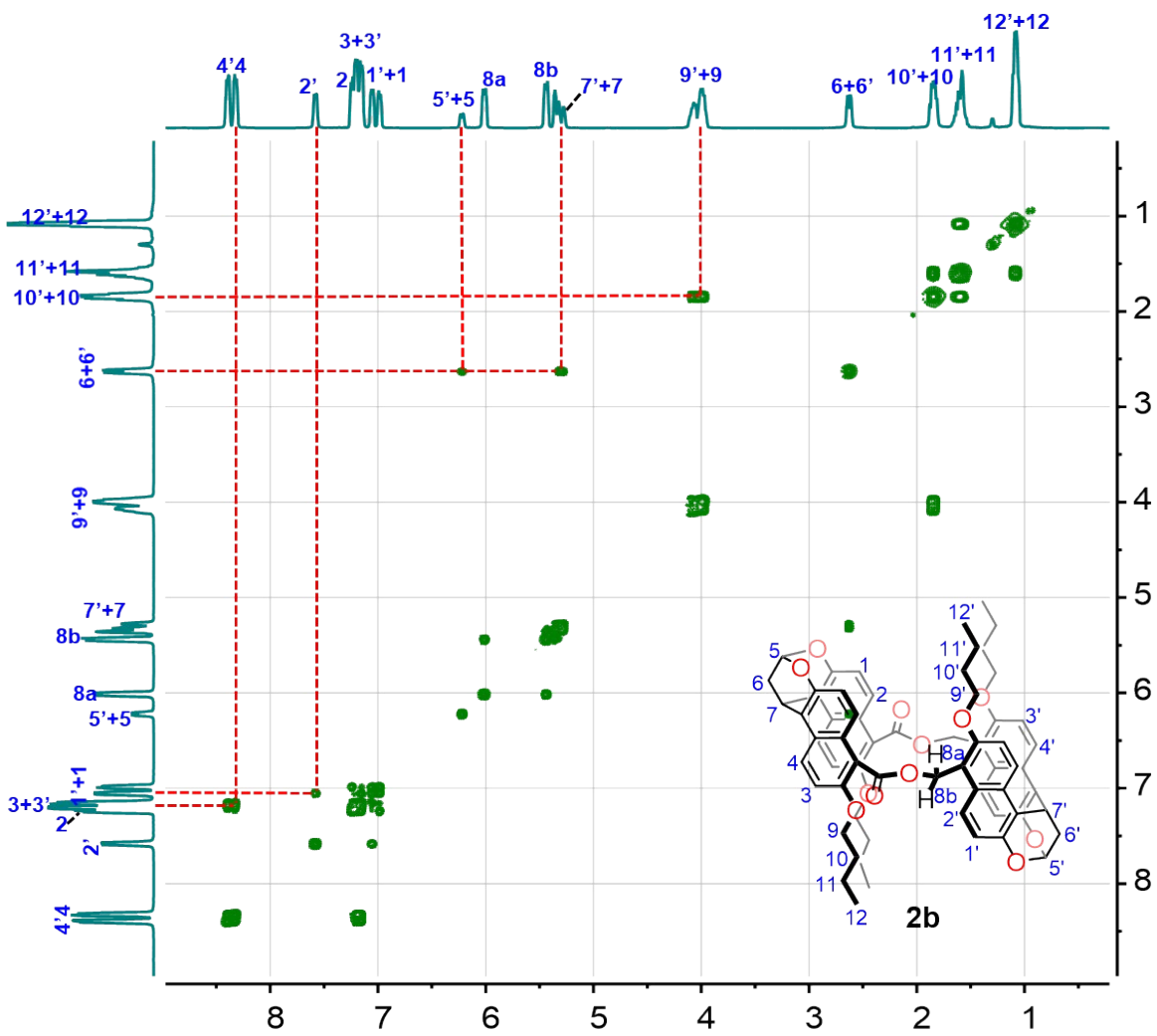


Fig. S4 ^1H , ^1H -COSY NMR spectrum (500 MHz, CD_2Cl_2 , 298 K) of **2b**.

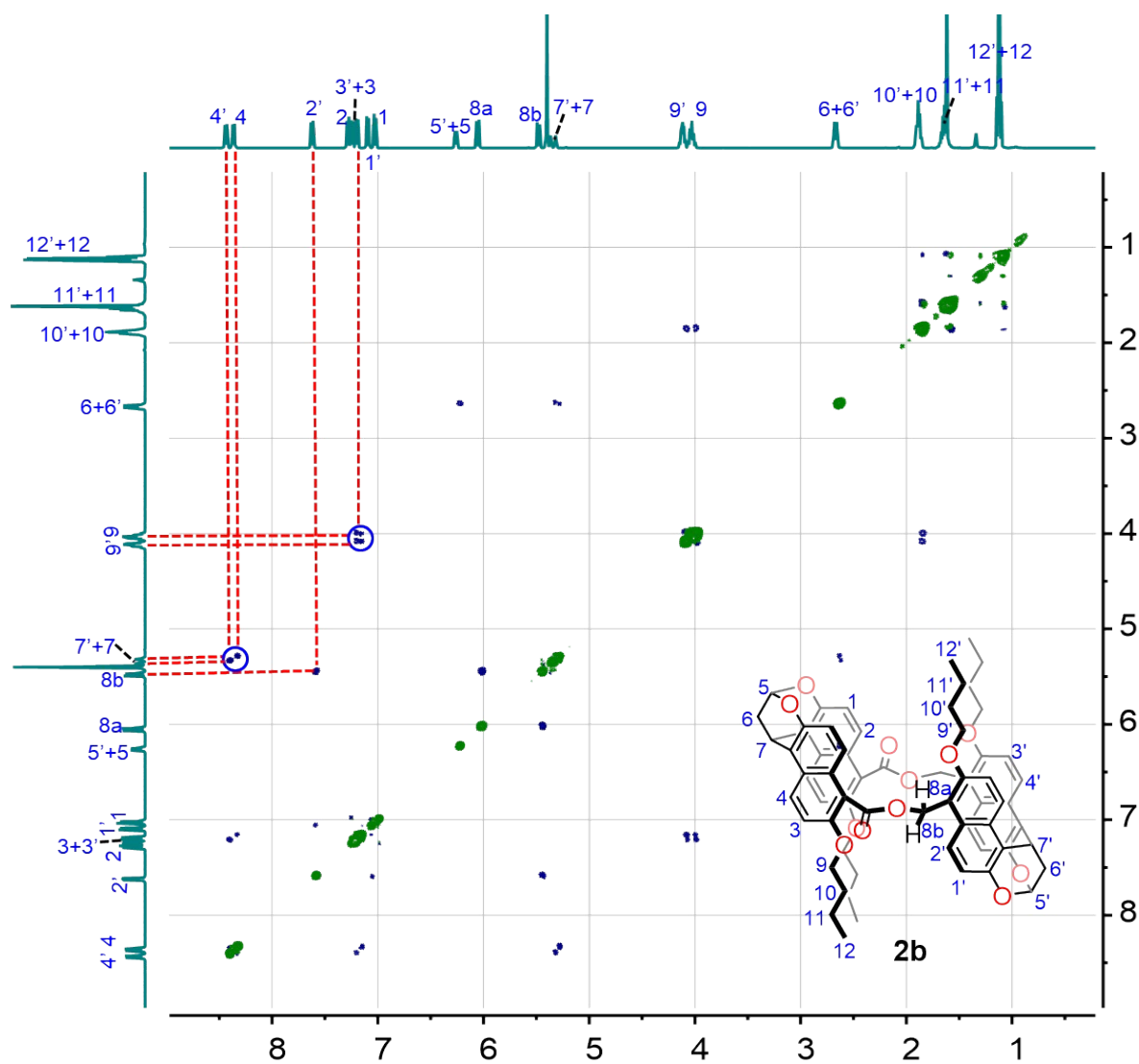


Fig. S5 $^1\text{H},^1\text{H}$ -ROESY NMR spectrum (500 MHz, CD_2Cl_2 , 298 K) of **2b**. No NOE effect was detected between the alkyl protons (9-12) and aromatic protons (1 and 2).

2. Characterization Data of Host-Guest Complexes

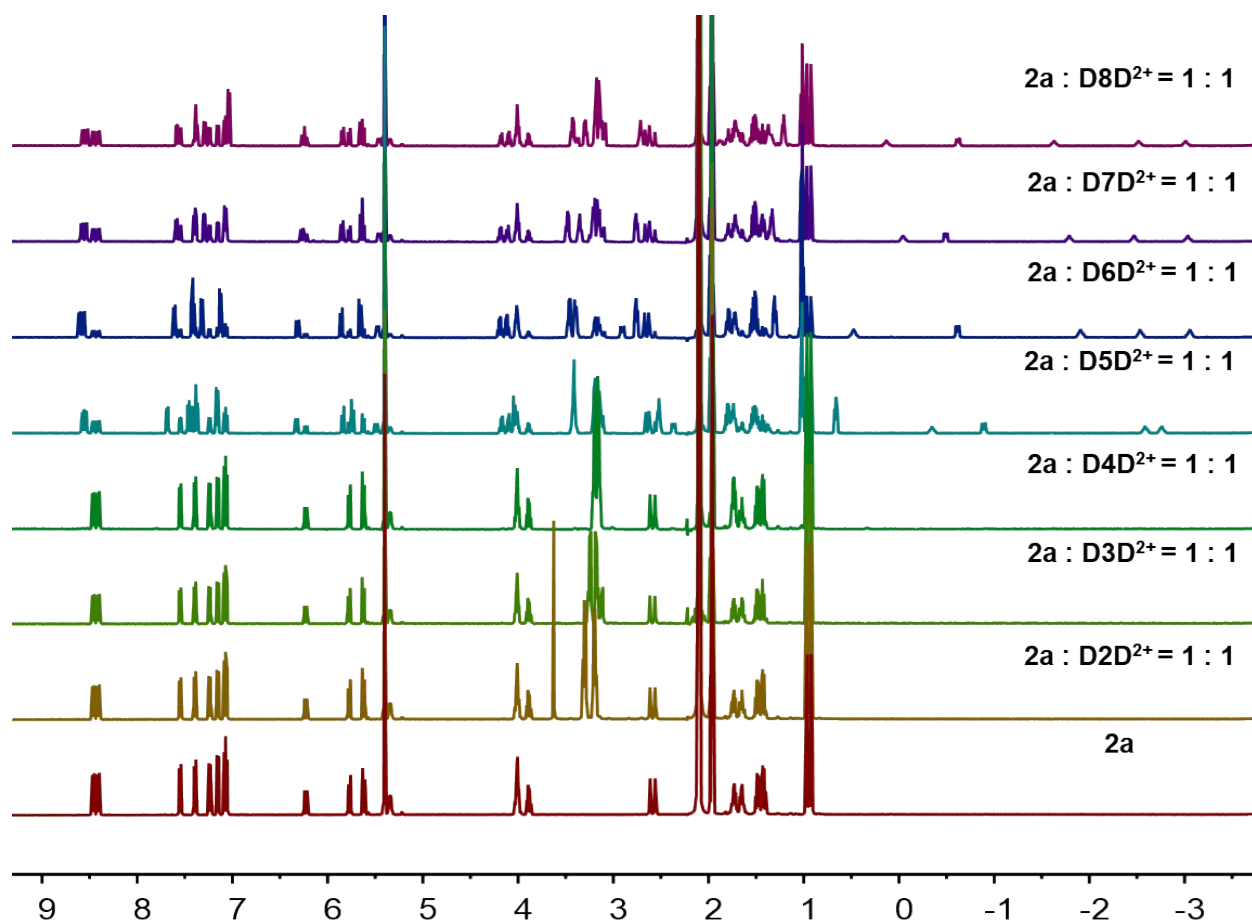


Fig. S6 Full ¹H NMR spectra (500 MHz, CD₂Cl₂:CD₃CN=1:1, 2.0 mM, 298 K) of **2a** in the absence or the presence of one equivalent of individual guest **D2D²⁺** - **D8D²⁺**. **2a** does not bind **D2D²⁺** - **D3D²⁺**, as indicated no obvious shift of both the guest and the host. For the guests **D4D²⁺** - **D8D²⁺**, the complexes are slow-exchanging at the NMR timescale. Therefore, the binding constants can be determined by integration method. In general, the binding constants are smaller than 10⁴ M⁻¹. Thus, these bindings are too weak to be determined by our Nano ITC instrument. These experiments together with peak integration indicate 1:1 binding stoichiometry between **2a** and the DABCO-based organic cations **D4D²⁺** - **D8D²⁺**.

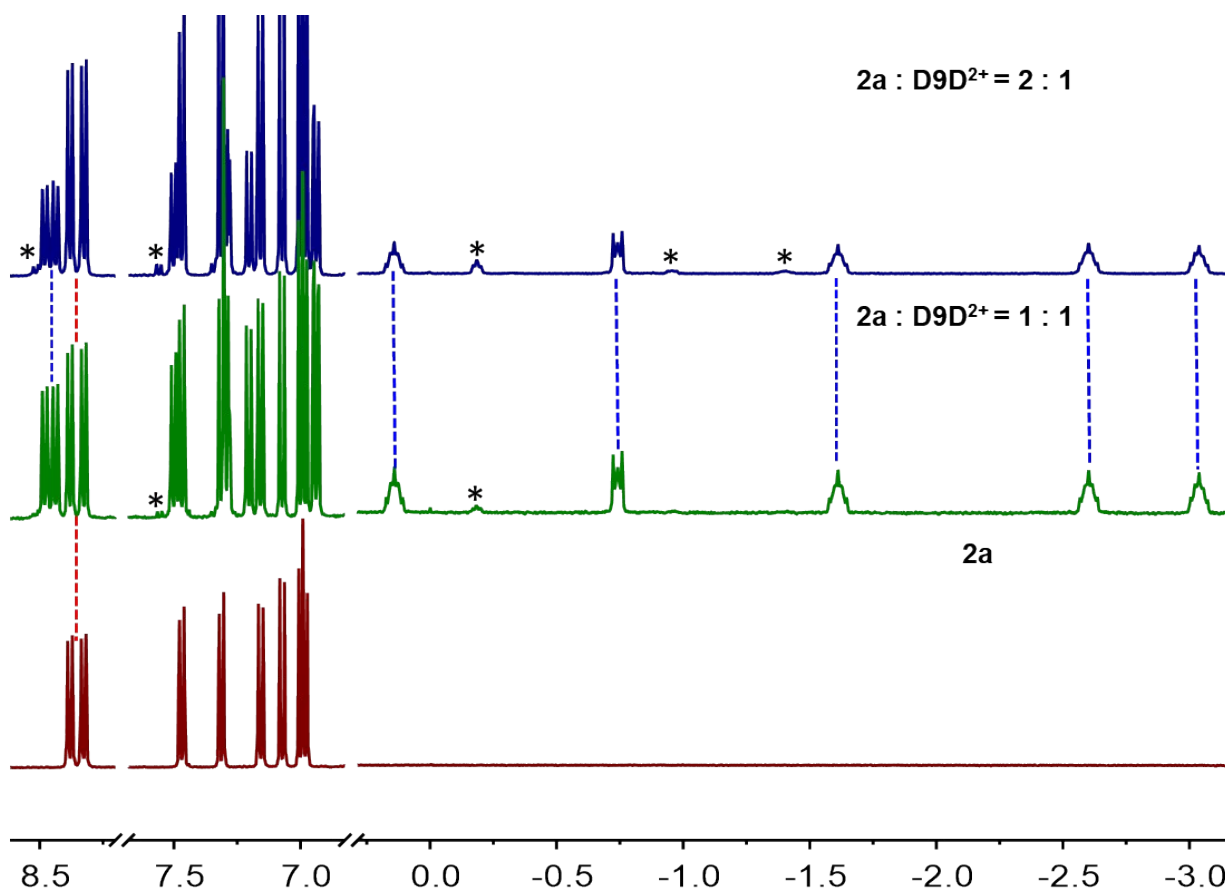


Fig. S7 Selected region of the ¹H NMR spectra (500 MHz, CD₂Cl₂ : CD₃CN = 1 : 1, 298 K) of **2a** and 1:1 and 2:1 mixture of **2a** with guest **D9D²⁺**. In the mixture of **2a** and **D9D²⁺**, free host and complex **D9D²⁺@2a** predominate. The 1:2 complex **D9D²⁺@2a₂** can be observed only in the presence of excess **2a** and exist in very small amount. “*” indicates complex **D9D²⁺@2a₂**.

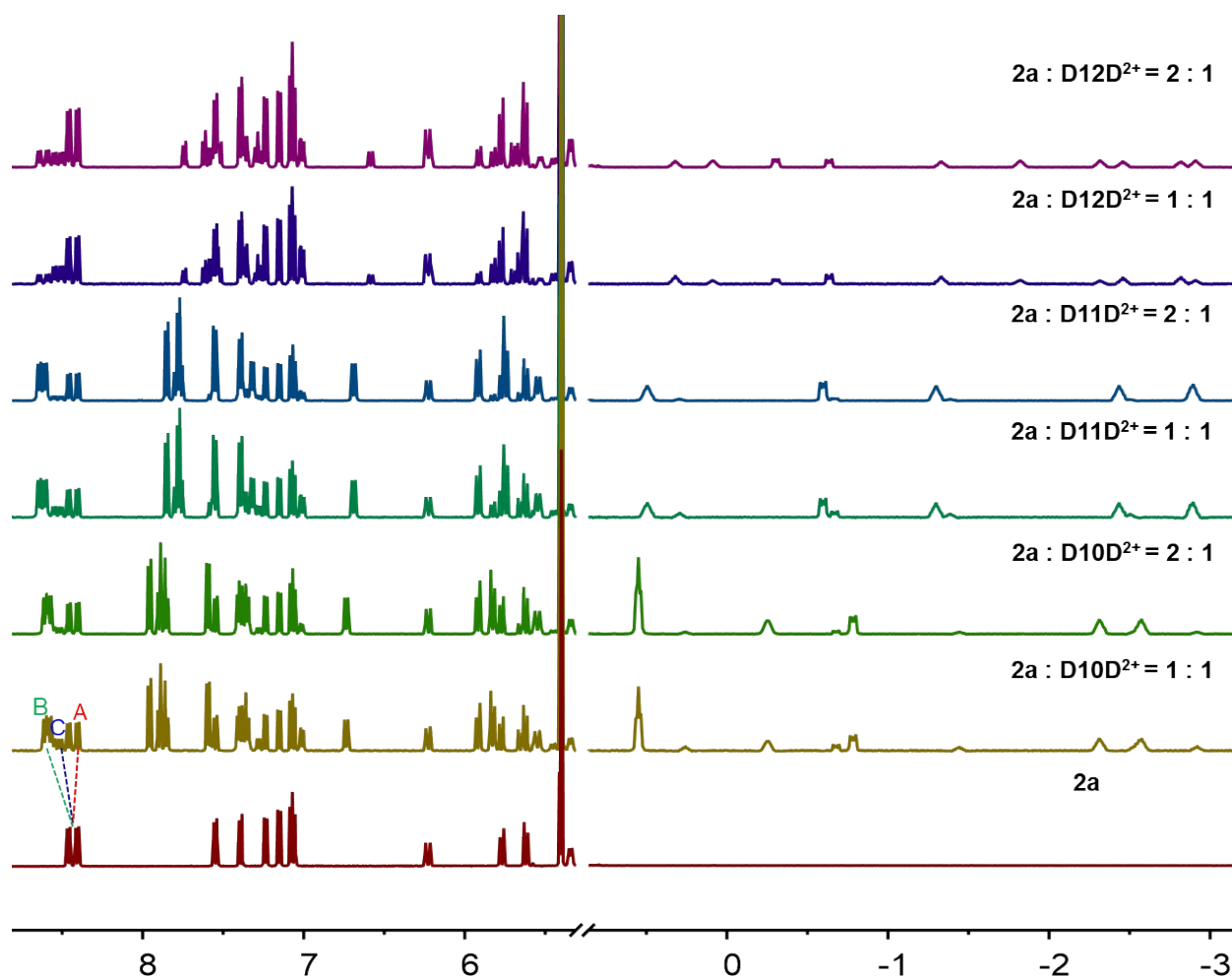


Fig. S8 Selected region of the ^1H NMR spectra (500 MHz, $\text{CD}_2\text{Cl}_2:\text{CD}_3\text{CN}=1:1$, 2.0 mM, 298 K) of **2a** and 1:1 and 2:1 mixture of **2a** with individual guest D10D^{2+} - D12D^{2+} . In the mixture of **2a** and different guests, there have some free host but two complexes were detected. They undergo stepwise binding with two **2a**. The one increased in the 2:1 mixtures is $\text{DnD}^{2+}@2\mathbf{a}_2$. **A**、**B** and **C** are used to denote free host (**A**), $\text{DnD}^{2+}@2\mathbf{a}_2$ (**B**), and $\text{DnD}^{2+}@2\mathbf{a}$ (**C**) respectively. The complexes are slow-exchanging at the NMR timescale, therefore, the stepwise binding constants can be determined by integration method. Notably, the 1:1 complex $\text{D10D}^{2+}@2\mathbf{a}$ and $\text{D11D}^{2+}@2\mathbf{a}$ only exist in very small amount in the 1:2 mixture of guest and host, while complex $\text{D10D}^{2+}@2\mathbf{a}_2$ and $\text{D11D}^{2+}@2\mathbf{a}_2$ predominates. This suggests the high stability and robustness of $\text{D10D}^{2+}@2\mathbf{a}_2$, $\text{D11D}^{2+}@2\mathbf{a}_2$, which originates from strong allosteric cooperativity.

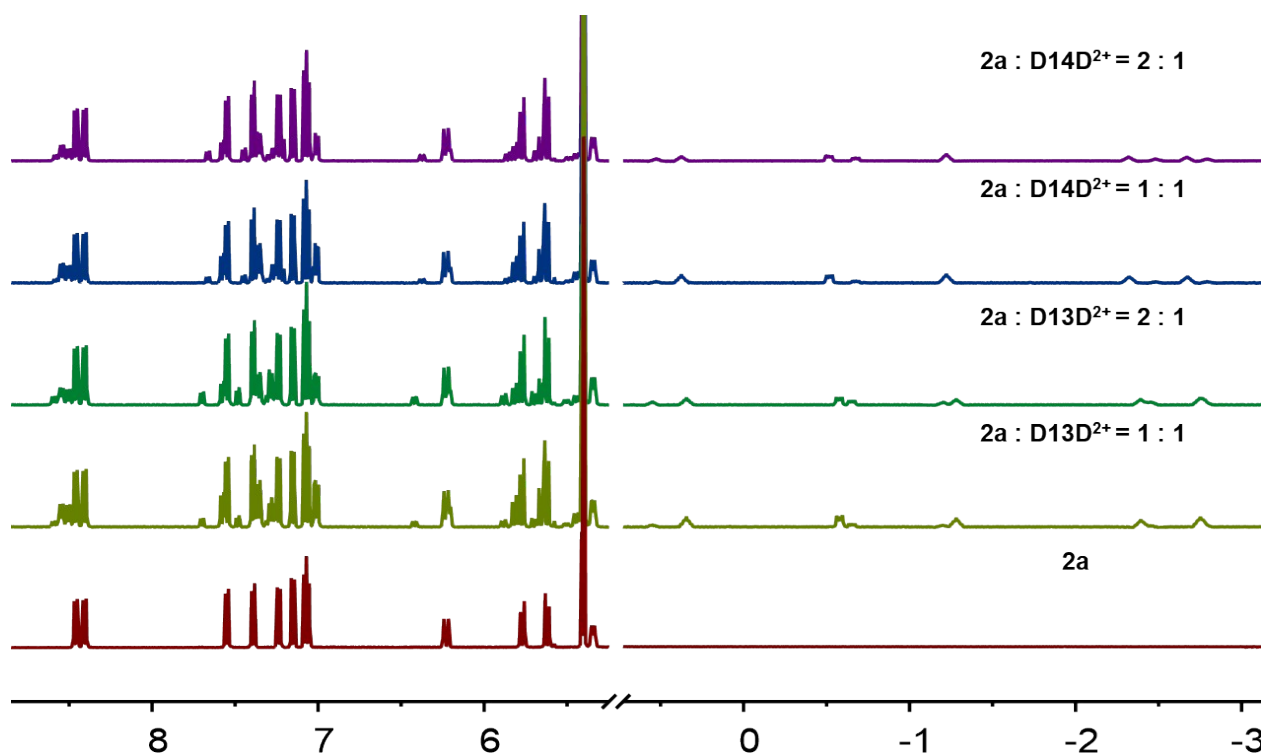


Fig. S9 Selected region of the ¹H NMR spectra (500 MHz, CD₂Cl₂:CD₃CN=1:1, 2.0 mM, 298 K) of **2a** and 1:1 and 2:1 mixture of **2a** with individual guest **D13D²⁺** - **D14D²⁺**. Similar phenomena as those for guests **D10D²⁺** - **D12D²⁺** were observed. Therefore, they also undergo stepwise binding with two **2a**. However, the 1:2 complex **DnD²⁺@2a₂** only exist in very small amount, the free host and complex **DnD²⁺@2a** predominate. This suggests **2a** form weak binding with **D13D²⁺** or **D14D²⁺** in 2:1 binding stoichiometry and no allosteric cooperativity.

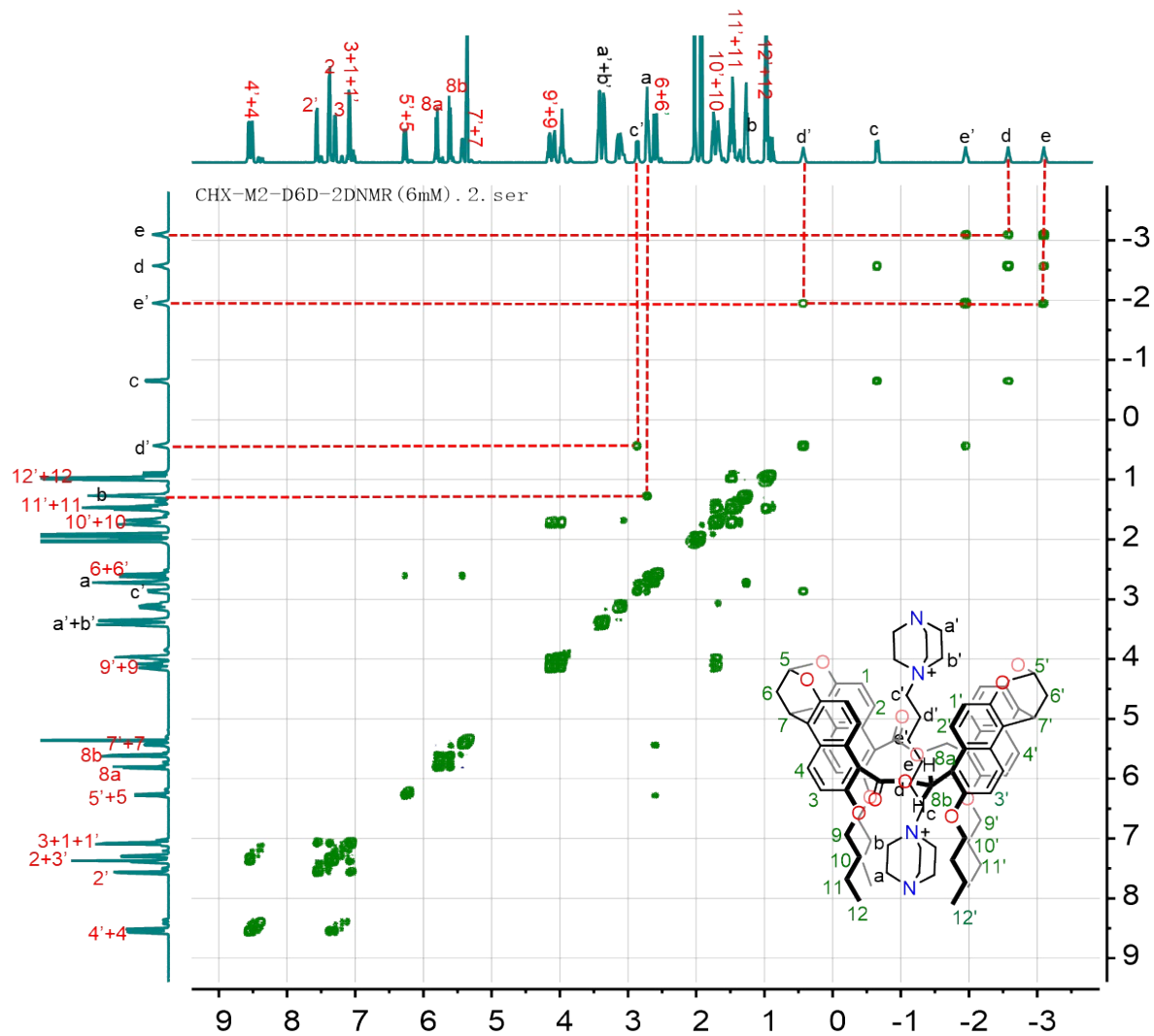


Fig. S10 $^1\text{H},^1\text{H}$ -COSY NMR spectrum (500 MHz, $\text{CD}_2\text{Cl}_2:\text{CD}_3\text{CN}=1:1$, 6.0 mM, 298 K) of $\text{D6D}^{2+}@2\mathbf{a}$.

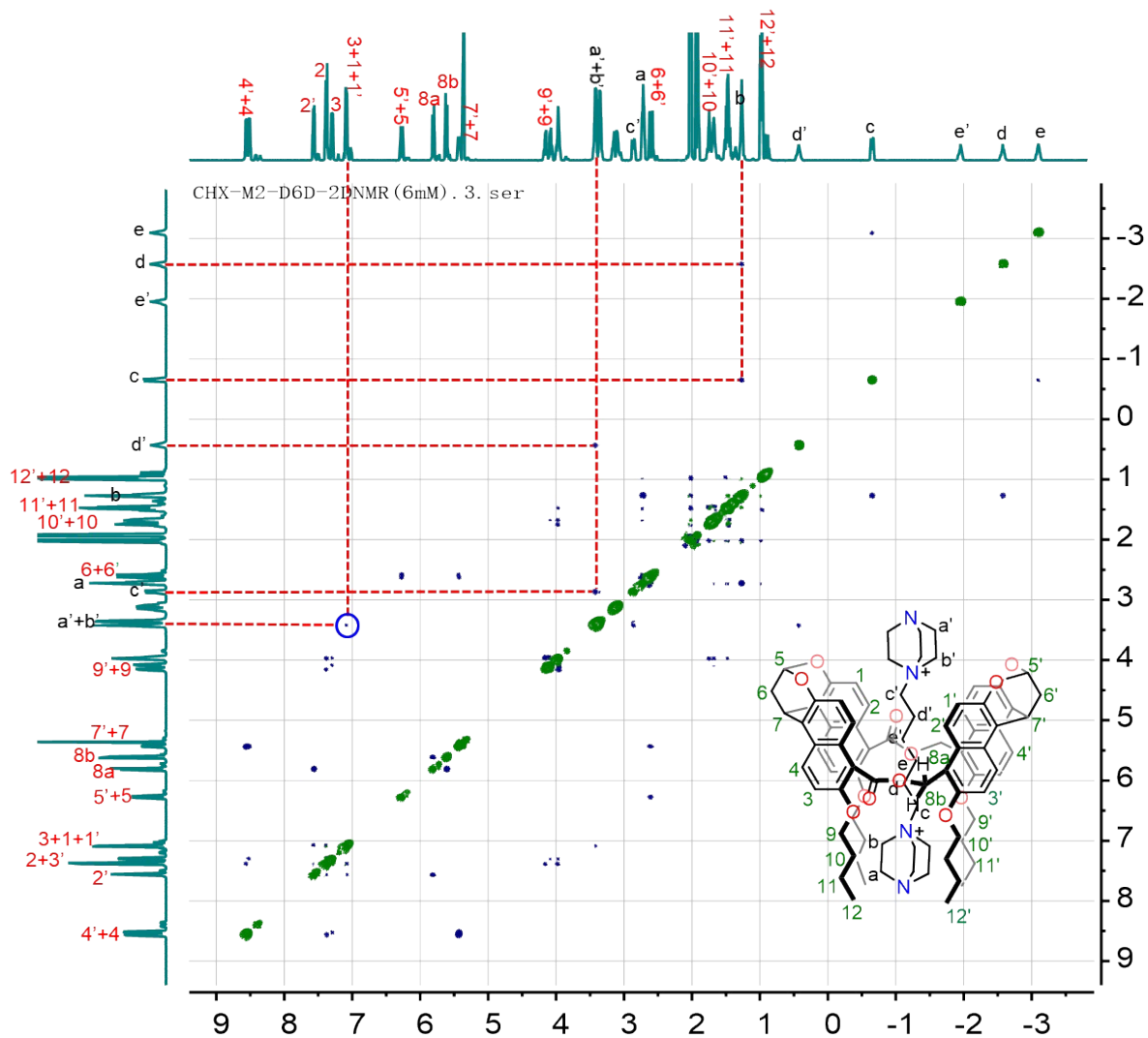


Fig. S11 $^1\text{H}, ^1\text{H}$ -ROESY NMR spectrum (500 MHz, $\text{CD}_2\text{Cl}_2:\text{CD}_3\text{CN}=1:1$, 6.0 mM, 298 K) of $\text{D6D}^{2+}@2\mathbf{a}$. All the peaks can unambiguously assigned according the COSY and ROESY NMR spectra. The NOE cross peaks of protons $\text{a}'+\text{b}'$ with protons $1+1'$ but not with proton 2 suggest that one of the DABCO protrudes the cavity. This is in line with the fact that one of DABCO undergo downfield shift in the complex.

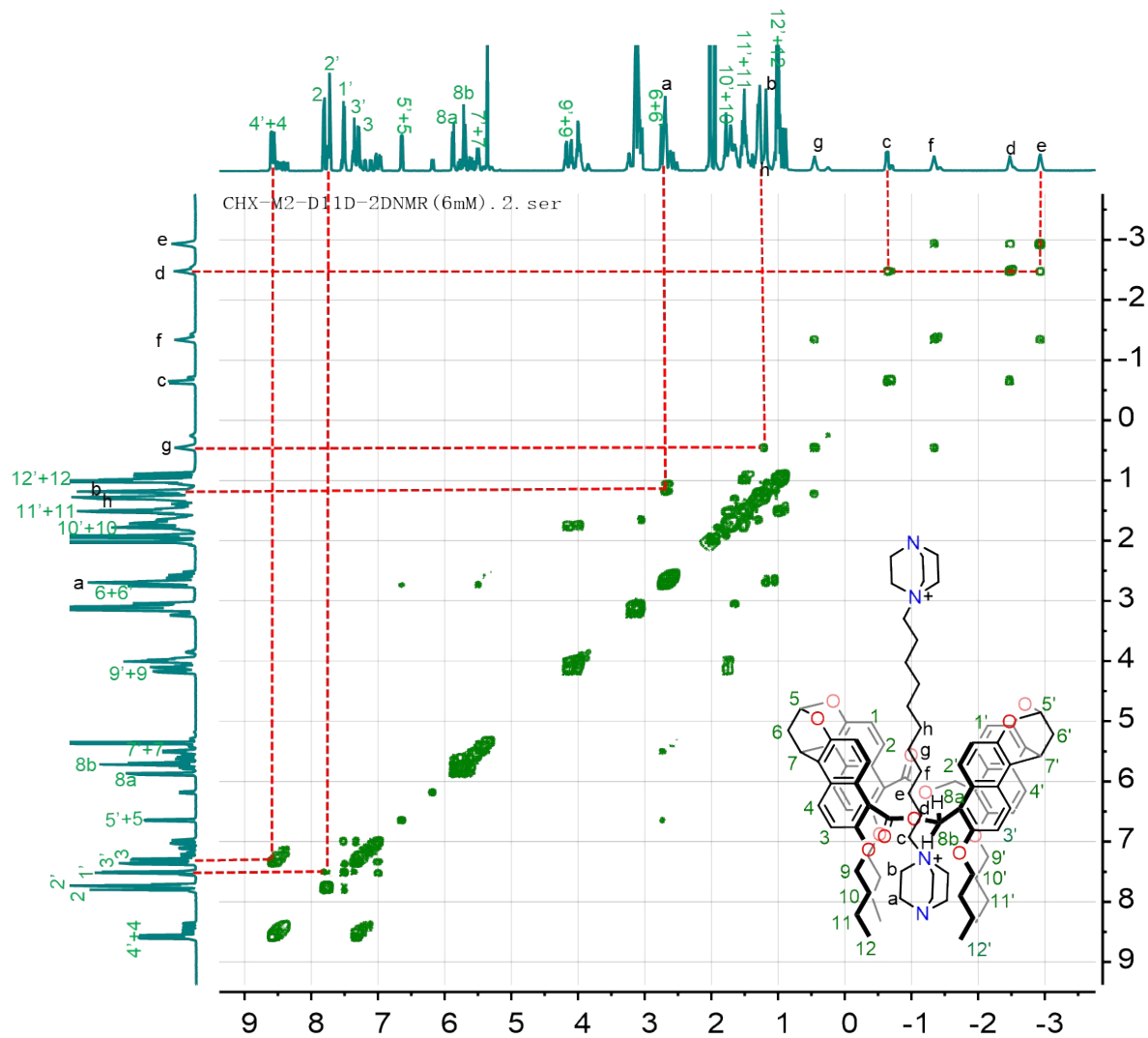


Fig. S12 $^1\text{H},^1\text{H}$ -COSY NMR spectrum (500 MHz, $\text{CD}_2\text{Cl}_2:\text{CD}_3\text{CN}=1:1$, 6.0 mM, 298 K) of **D11D $^{2+}$ @2a**.

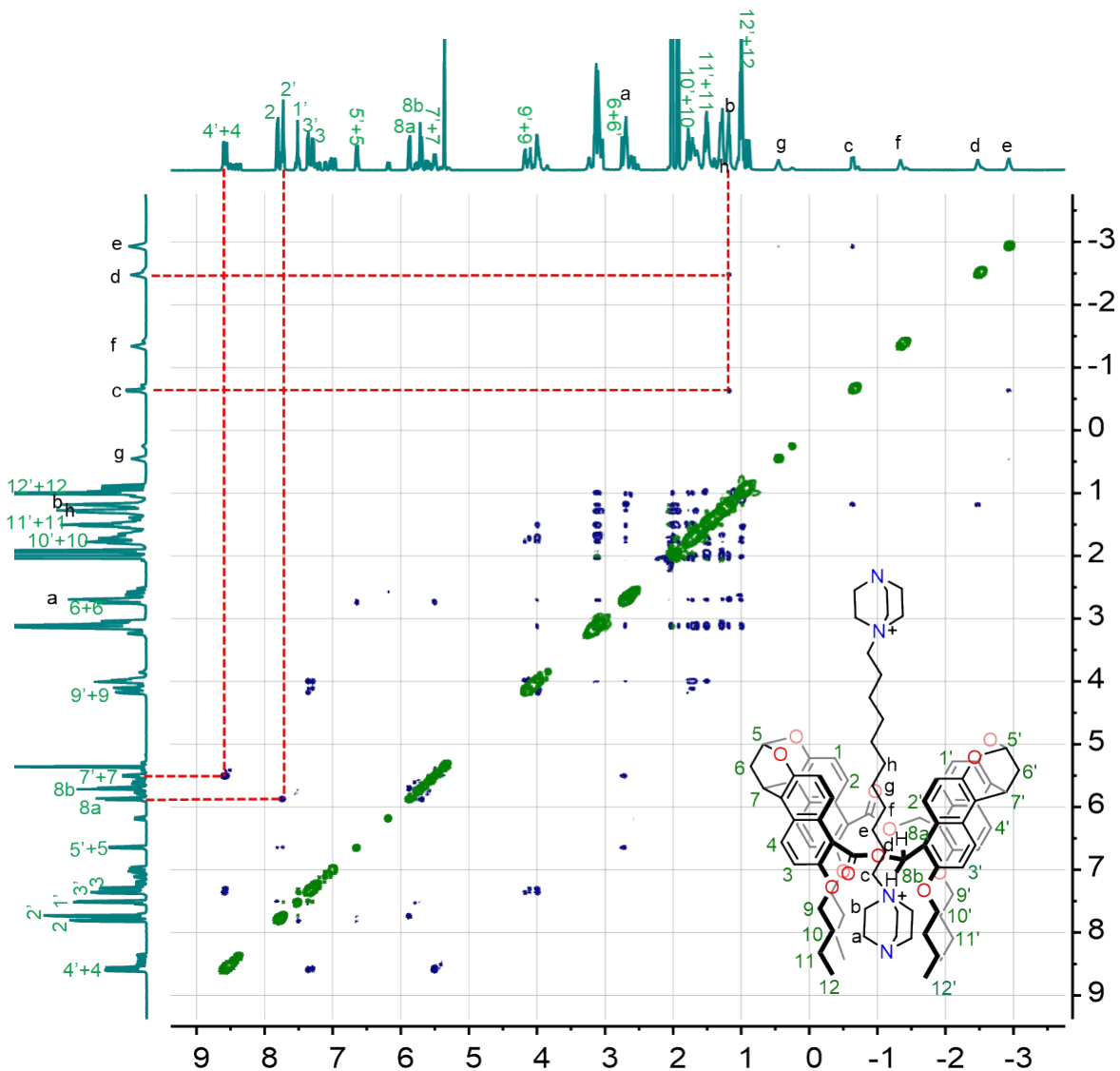


Fig. S13 $^1\text{H},^1\text{H}$ -ROESY NMR spectrum (500 MHz, $\text{CD}_2\text{Cl}_2:\text{CD}_3\text{CN}=1:1$, 6.0 mM, 298 K) of **D11D $^{2+}$ @2a**. All the peaks can unambiguously assigned according the COSY and ROESY NMR spectra. No NOE contact between proton of DABCO and the host was detected.

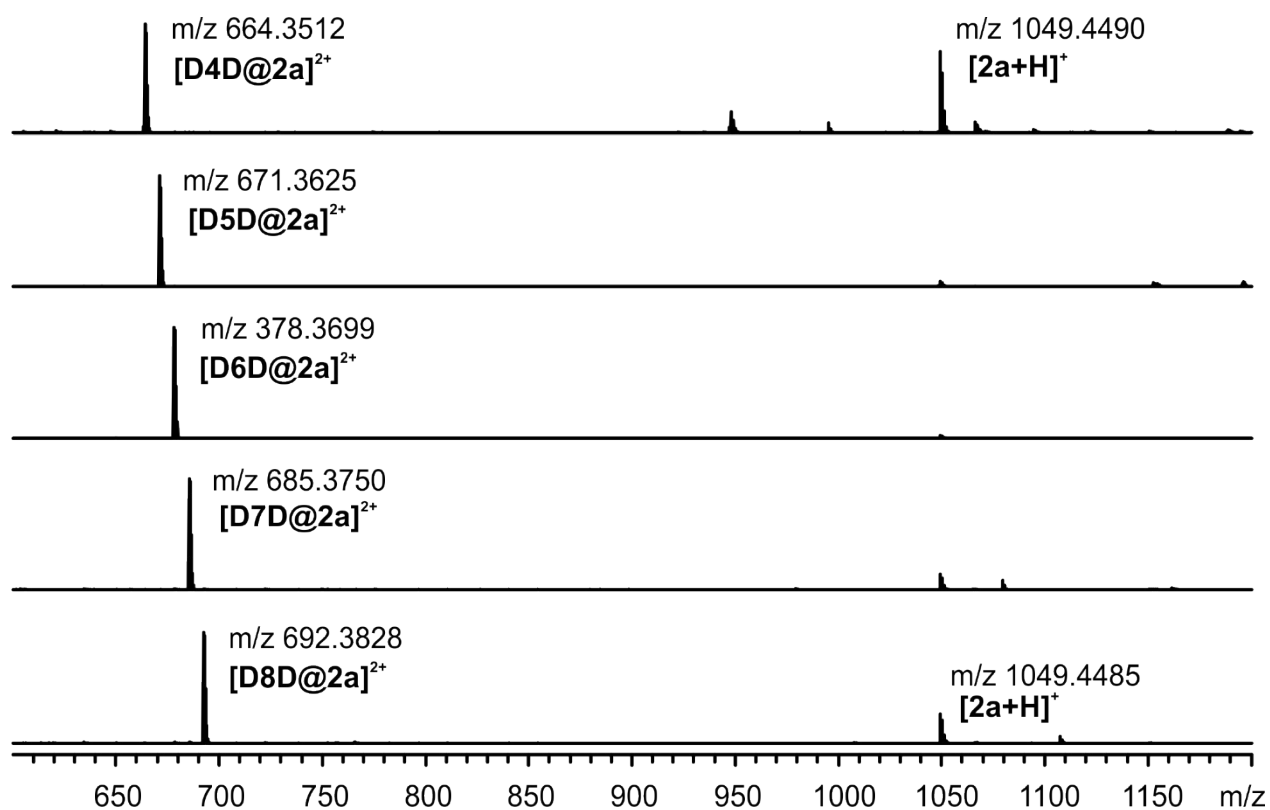


Fig. S14 Mass spectra of **D4D**²⁺@**2a** – **D8D**²⁺@**2a** in the mixture of CH₃CN and CH₂Cl₂ (1:10). The peaks assigned to the corresponding 1:1 complexes and free host **2a** were detected, suggesting **2a** binds with these DABCO guests in 1:1 binding stoichiometry.

The association constants which were calculated by single-point method:



$$K_1 = \frac{[G@H]}{[G] \cdot [H]} \quad K_2 = \frac{[G@H_2]}{[G@H] \cdot [H]}$$

$$\text{Cooperativity factor } (\alpha): \quad \alpha = 4K_1/K_2$$

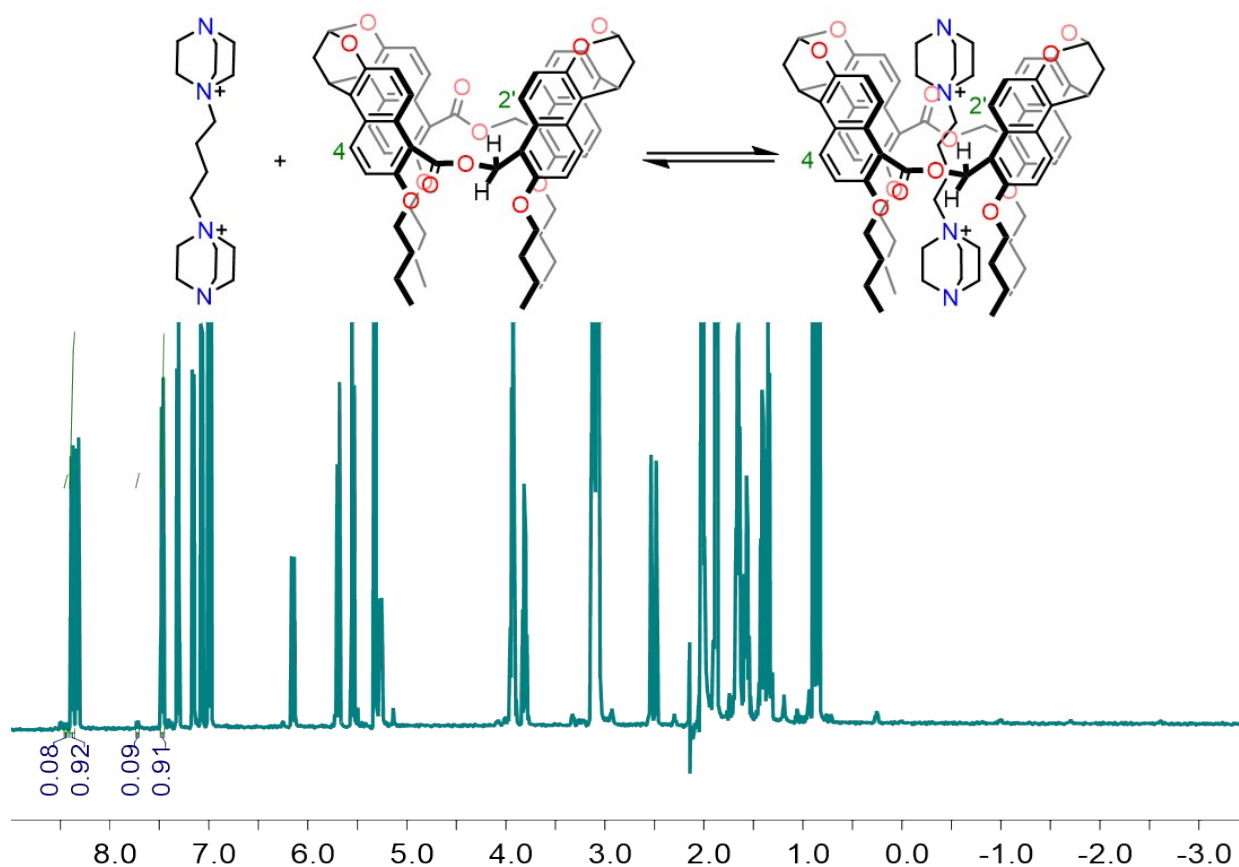


Fig. S15 ^1H NMR spectrum (500 MHz, 298 K, $\text{CDCl}_3:\text{CD}_3\text{CN} = 1:1$, 2.0 mM) of the equimolar mixture of D4D^{2+} and **2a**. From complexed and uncomplexed H_2' and H_4 of **2a**, $K_a(\text{H}_4) = [0.08 \times 2.0 \times 10^{-3}] / [0.92 \times 2.0 \times 10^{-3}] / [2.0 \times 10^{-3} - 0.08 \times 2.0 \times 10^{-3}] \text{ M}^{-1} = 47 \text{ M}^{-1}$; $K_a(\text{H}_2') = [0.09 \times 2.0 \times 10^{-3}] / [0.91 \times 2.0 \times 10^{-3}] / [2.0 \times 10^{-3} - 0.09 \times 2.0 \times 10^{-3}] \text{ M}^{-1} = 54 \text{ M}^{-1}$. Finally, $K_a = (47 + 54) / 2 = 50 (\pm 5) \text{ M}^{-1}$.

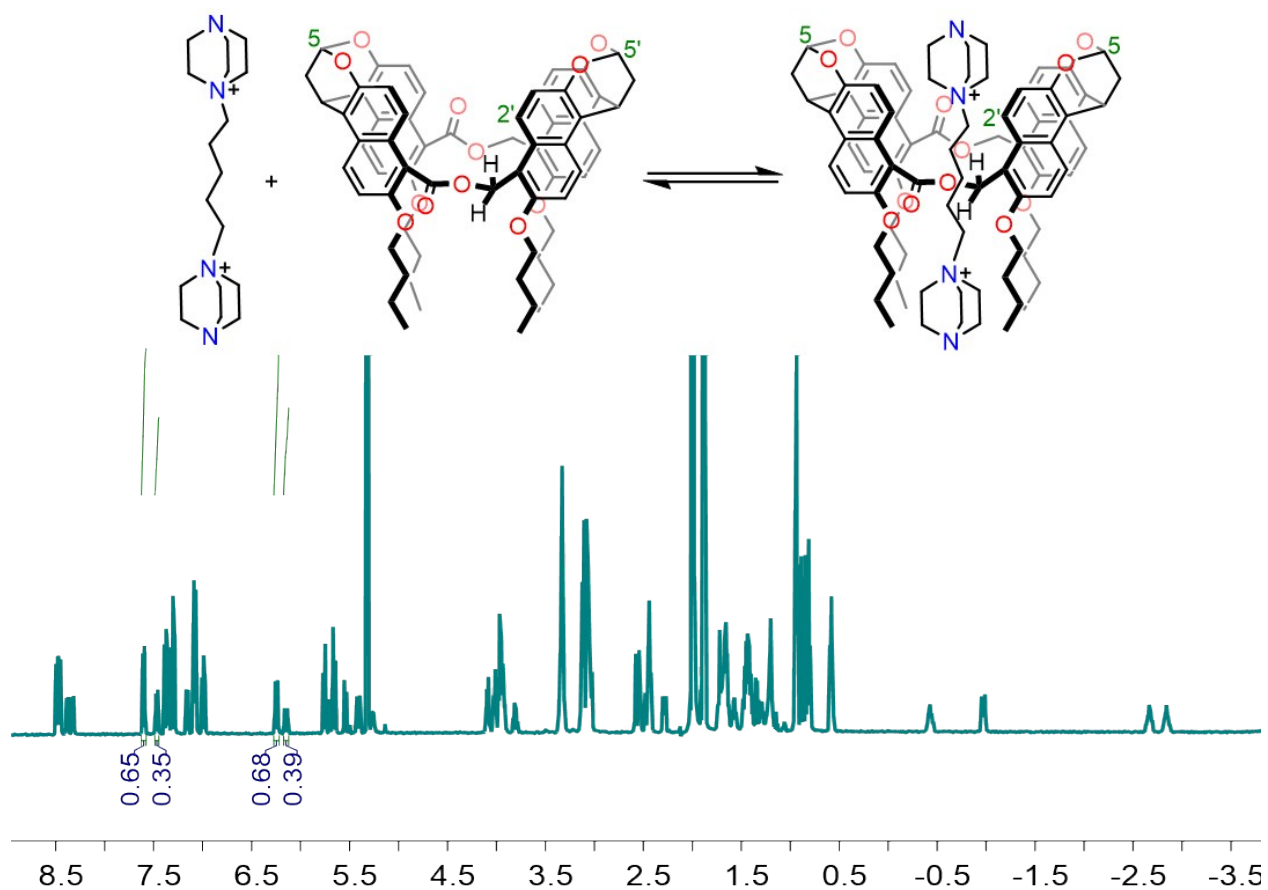


Fig. S16 1H NMR spectrum (500 MHz, 298 K, $CDCl_3:CD_3CN = 1:1$, 2.0 mM) of the equimolar mixture of $D5D^{2+}$ and **2a**. From complexed and uncomplexed $H_{2'}$ and $H_{5+5'}$ of **2a**, $K_a(H_{2'}) = [0.65 \times 2.0 \times 10^{-3}] / [0.35 \times 2.0 \times 10^{-3}] / [(2.0 \times 10^{-3} - 0.65 \times 2.0 \times 10^{-3})] M^{-1} = 2653 M^{-1}$; $K_a(H_{5+5'}) = [(0.68/1.07) \times 2.0 \times 10^{-3}] / [(0.39/1.07) \times 2.0 \times 10^{-3}] / [(2.0 \times 10^{-3} - (0.68/1.07) \times 2.0 \times 10^{-3})] M^{-1} = 2492 M^{-1}$. Finally, $K_a = (2653 + 2492) / 2 = 2572 (\pm 114) M^{-1}$.

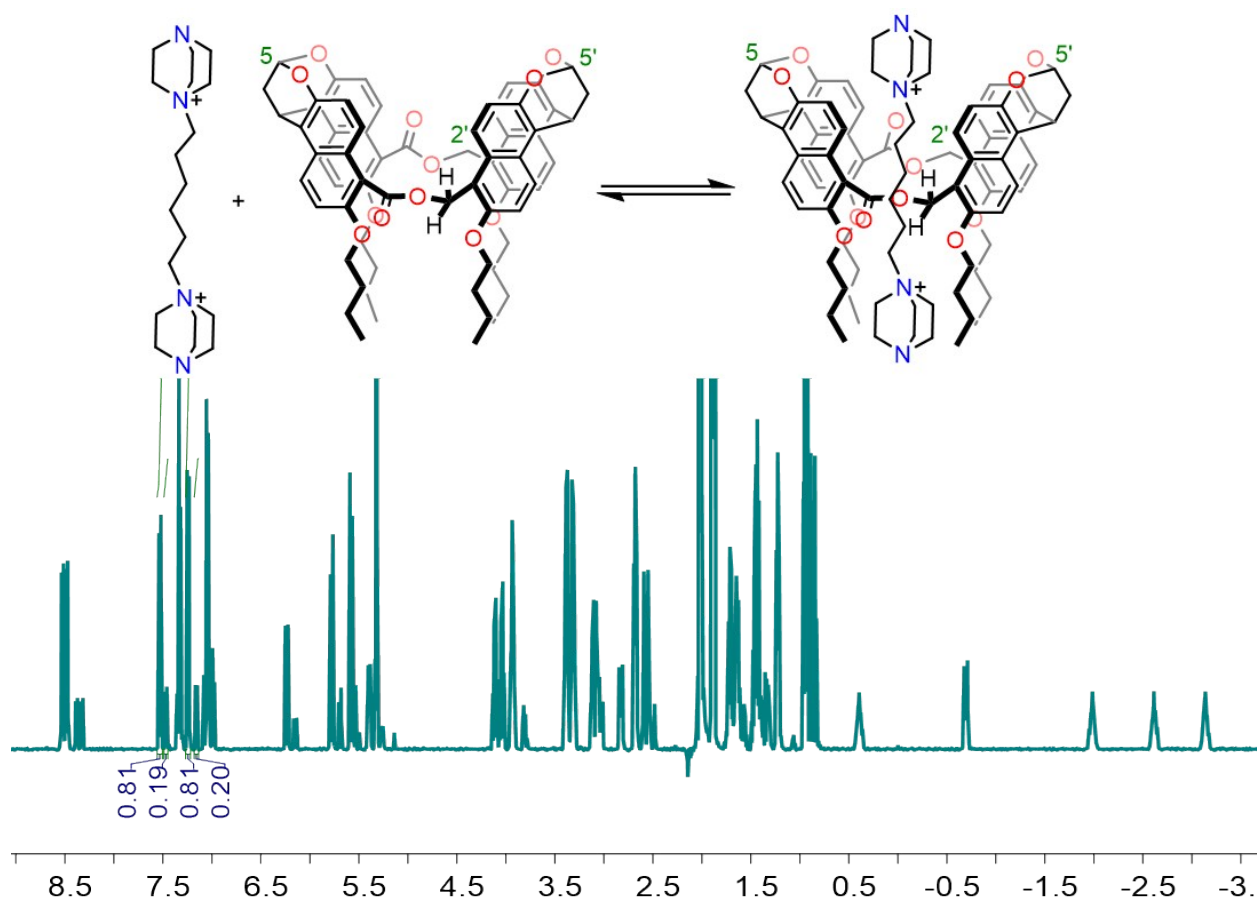


Fig. S17 ^1H NMR spectrum (500 MHz, 298 K, $\text{CDCl}_3:\text{CD}_3\text{CN} = 1:1$, 2.0 mM) of the equimolar mixture of $D6D^{2+}$ and **2a**. From complexed and uncomplexed H_2 and $\text{H}_{5+5'}$ of **2a**, $K_a(\text{H}_2) = [(0.81 \times 2.0 \times 10^{-3}) / [0.19 \times 2.0 \times 10^{-3}] / [2.0 \times 10^{-3} - 0.81 \times 2.0 \times 10^{-3}]] \text{ M}^{-1} = 11219 \text{ M}^{-1}$; $K_a(\text{H}_{5+5'}) = [0.81 \times 2.0 \times 10^{-3}] / [0.20 \times 2.0 \times 10^{-3}] / [2.0 \times 10^{-3} - 0.81 \times 2.0 \times 10^{-3}] \text{ M}^{-1} = 10658 \text{ M}^{-1}$. Finally, $K_a = (11219 + 10658) / 2 = 10938 (\pm 397) \text{ M}^{-1}$.

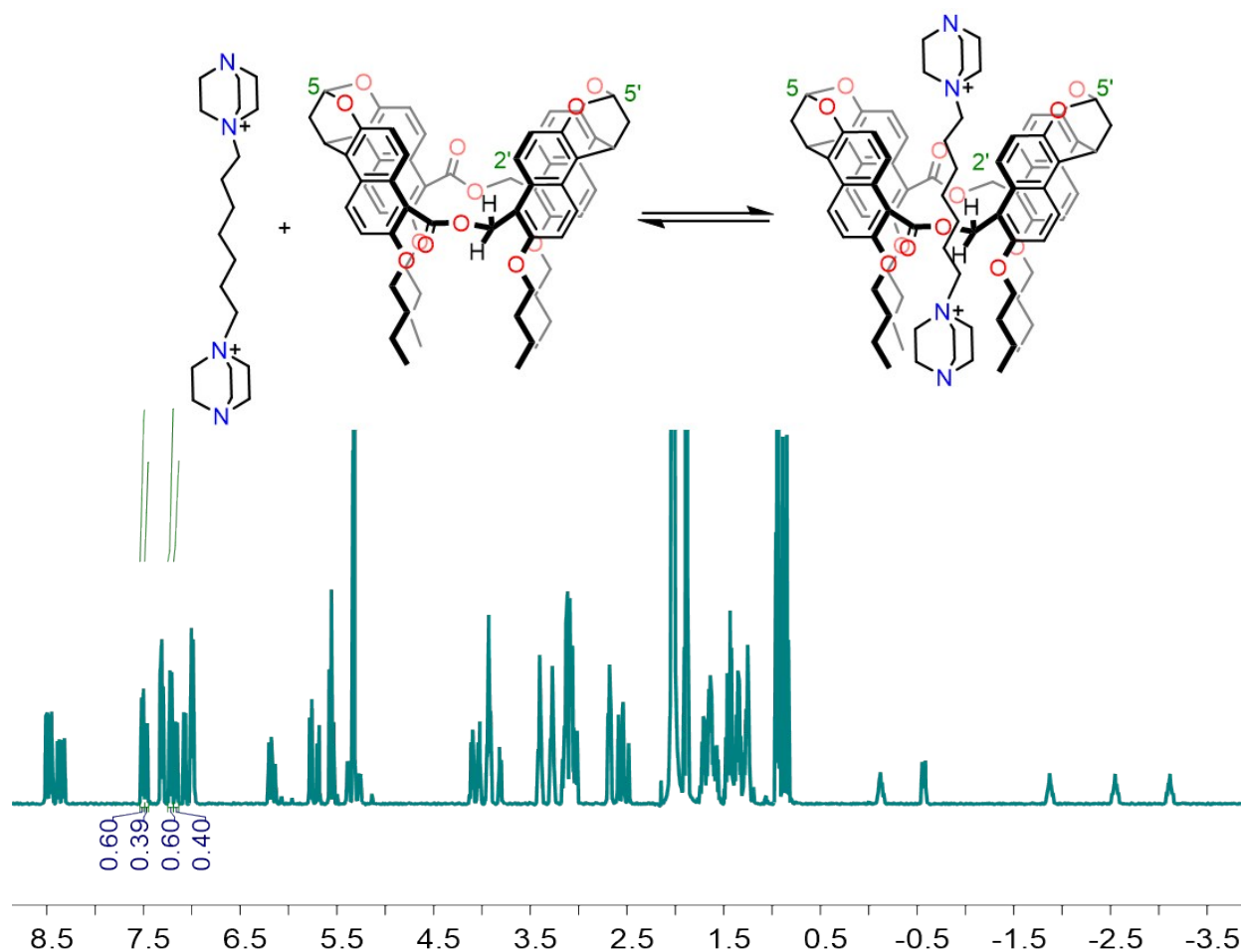


Fig. S18 ^1H NMR spectrum (500 MHz, 298 K, $\text{CDCl}_3:\text{CD}_3\text{CN} = 1:1$, 2.0 mM) of the equimolar mixture of D7D^{2+} and **2a**. From complexed and uncomplexed $\text{H}_{2'}$ and $\text{H}_{5+5'}$ of **2a**, $K_a(\text{H}_{2'}) = [(0.60/0.99) \times 2.0 \times 10^{-3}] / [(0.39/0.99) \times 2.0 \times 10^{-3}] / [2.0 \times 10^{-3} - (0.60/0.99) \times 2.0 \times 10^{-3}] \text{ M}^{-1} = 1923 \text{ M}^{-1}$; $K_a(\text{H}_{5+5'}) = [0.60 \times 2.0 \times 10^{-3}] / [0.40 \times 2.0 \times 10^{-3}] / [2.0 \times 10^{-3} - 0.60 \times 2.0 \times 10^{-3}] \text{ M}^{-1} = 1875 \text{ M}^{-1}$. Finally, $K_a = (1923 + 1875) / 2 = 1899 (\pm 34) \text{ M}^{-1}$.

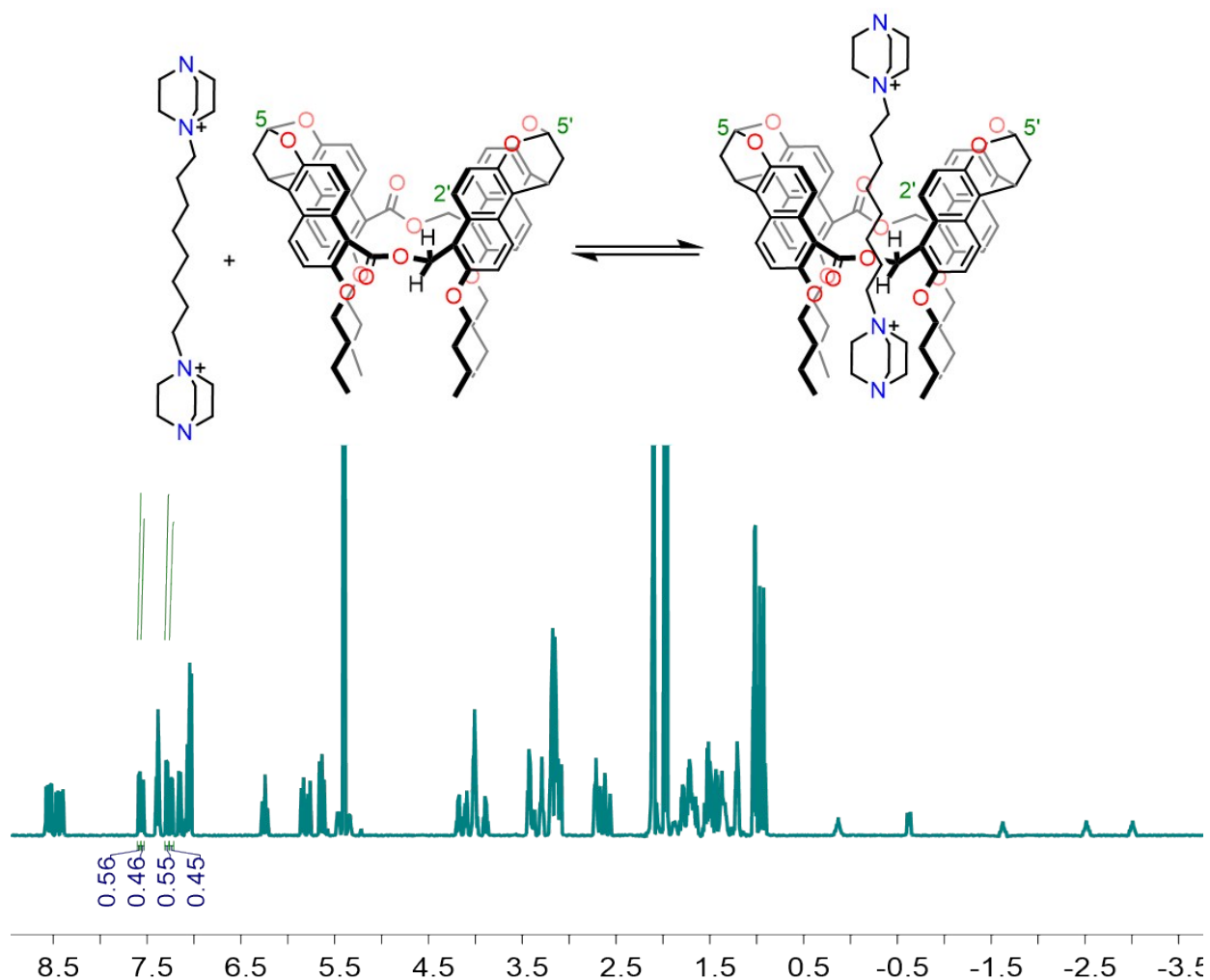


Fig. S19 ¹H NMR spectrum (500 MHz, 298 K, CDCl₃:CD₃CN = 1:1, 2.0 mM) of the equimolar mixture of D8D²⁺ and **2a**. From complexed and uncomplexed H_{2'} and H_{5+5'} of **2a**, $K_a(\text{H}_{2'}) = [0.56 \times 2.0 \times 10^{-3}] / [0.46 \times 2.0 \times 10^{-3}] / [2.0 \times 10^{-3} - 0.56 \times 2.0 \times 10^{-3}] \text{ M}^{-1} = 1383 \text{ M}^{-1}$; $K_a(\text{H}_{5+5'}) = [0.55 \times 2.0 \times 10^{-3}] / [0.45 \times 2.0 \times 10^{-3}] / [2.0 \times 10^{-3} - 0.55 \times 2.0 \times 10^{-3}] \text{ M}^{-1} = 1358 \text{ M}^{-1}$. Finally, $K_a = (1383 + 1358) / 2 = 1371 (\pm 19) \text{ M}^{-1}$.

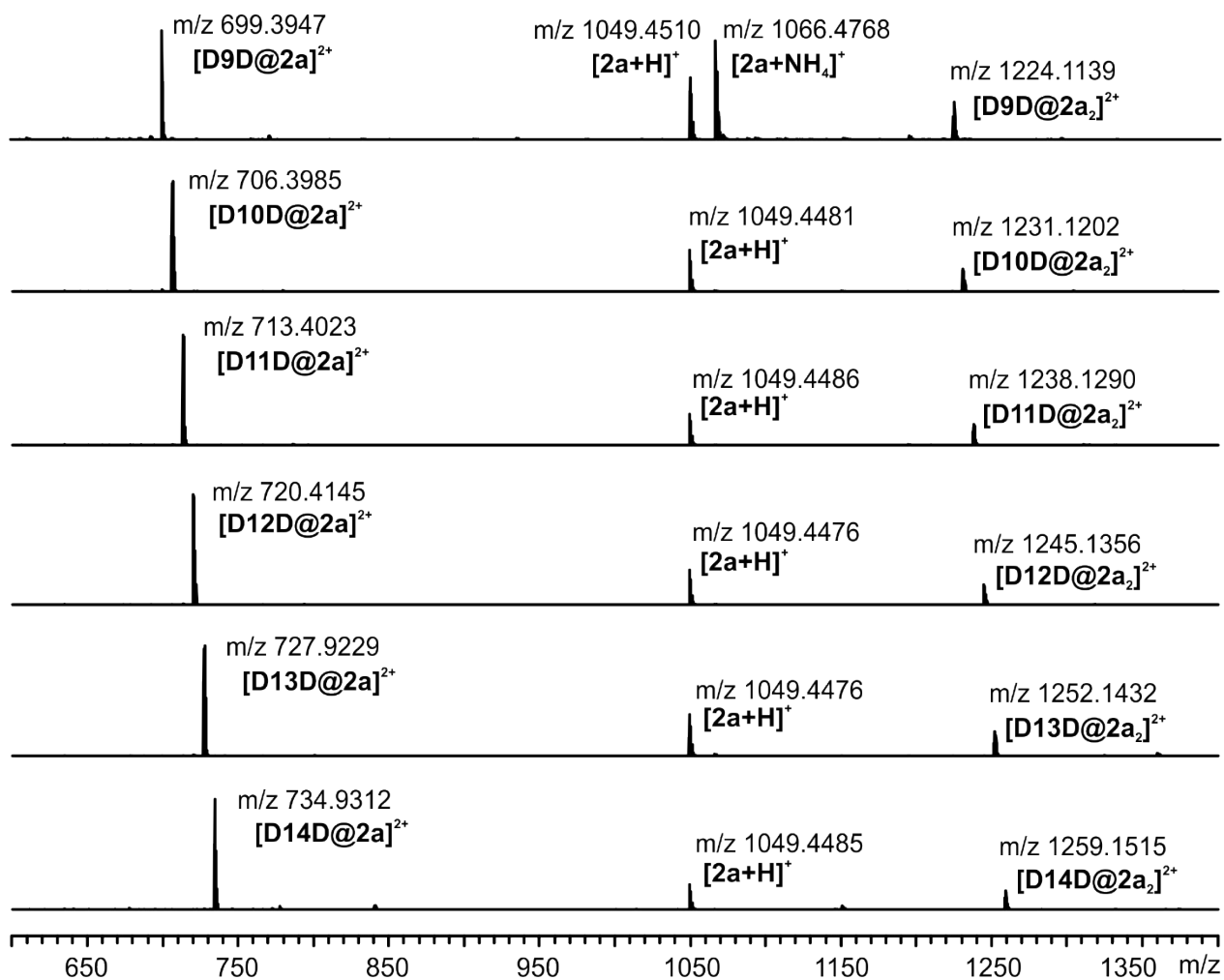


Fig. S20 Mass spectra of $D9D^{2+}@2a$ – $D14D^{2+}@2a$ in the mixture of CH_3CN and CH_2Cl_2 (1:10). The peaks assigned to the corresponding 1:1, 2:1 complexes and free host **2a** were detected, suggesting **2a** binds with these DABCO guests both in 1:1 and 2:1 binding stoichiometry.

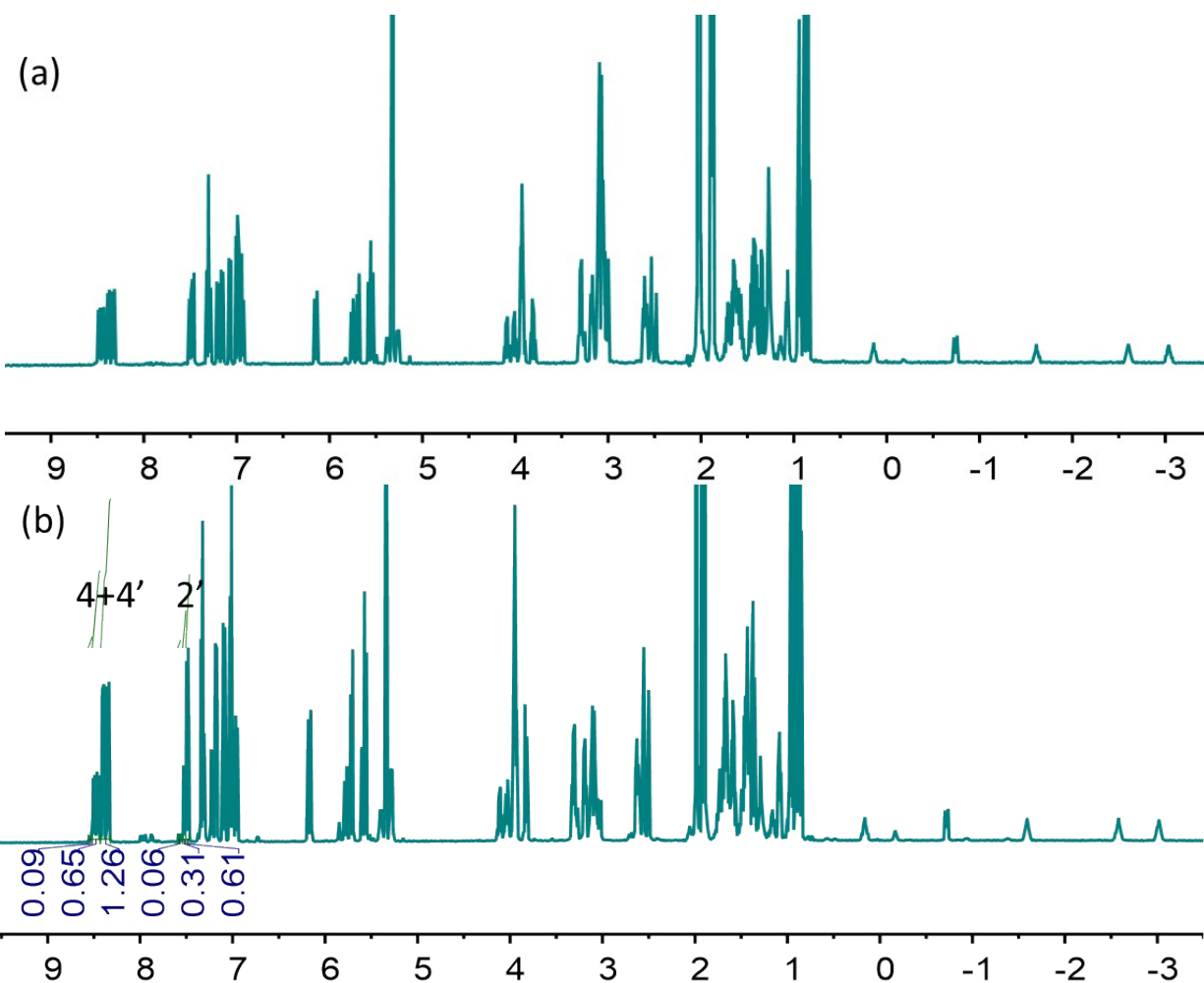


Fig. S21 ¹H NMR spectrum (500 MHz, 298 K, CDCl₃:CD₃CN = 1:1, 2.0 mM) of (a) the 1:1 mixture of **D9D**²⁺ and **2a** and (b) the 1:2 mixture of **D9D**²⁺ and **2a**. It is quite difficult to accurately determine the stepwise binding constants in 1:1 mixture of **D9D**²⁺ and **2a** since the complex **D9D**²⁺@**2a**₂ only exist in very small amount. In figure (b), from complexed and uncomplexed H_{4+4'} and H_{2'} of **2a**, $K_1(\text{H}_{4+4'}) = [(0.65 / 2.00) \times 4.0 \times 10^{-3}] / [(1.26 / 2.00) \times 4.0 \times 10^{-3}] / [4.0 \times 10^{-3} - (0.65 / 2.00) \times 4.0 \times 10^{-3} - (0.09 / 2.00) \times 4.0 \times 10^{-3} / 2] \text{ M}^{-1} = 846 \text{ M}^{-1}$; $K_2(\text{H}_{4+4'}) = [(0.09 / 2.00) \times 4.0 \times 10^{-3} / 2] / [(0.65 / 2.00) \times 4.0 \times 10^{-3}] / [(0.65 / 2.00) \times 4.0 \times 10^{-3}] \text{ M}^{-1} = 27 \text{ M}^{-1}$; $K_1(\text{H}_{2'}) = [(0.31 / 0.98) \times 4.0 \times 10^{-3}] / [(0.61 / 0.98) \times 4.0 \times 10^{-3}] / [4.0 \times 10^{-3} - (0.31 / 0.98) \times 4.0 \times 10^{-3} - (0.06 / 0.98) \times 4.0 \times 10^{-3} / 2] \text{ M}^{-1} = 830 \text{ M}^{-1}$; $K_2(\text{H}_{2'}) = [(0.06 / 0.98) \times 4.0 \times 10^{-3} / 2] / [(0.31 / 0.98) \times 4.0 \times 10^{-3}] / [(0.61 / 0.98) \times 4.0 \times 10^{-3}] \text{ M}^{-1} = 39 \text{ M}^{-1}$; Finally, $K_1 = (846 + 830) / 2 = 838 (\pm 11) \text{ M}^{-1}$, $K_2 = (27 + 39) / 2 = 33 (\pm 8) \text{ M}^{-1}$, $\alpha = 4K_2 / K_1 = 4 \times 33 / 838 = 0.16$.

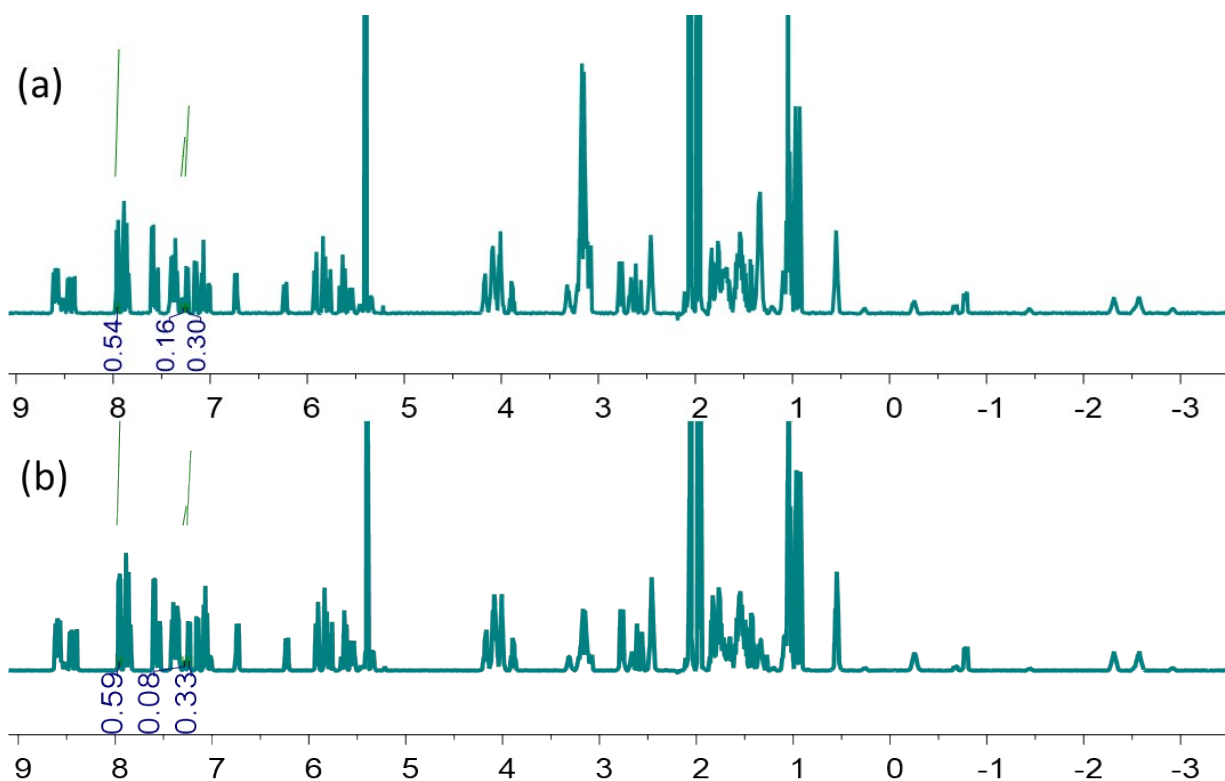


Fig. S22 ^1H NMR spectrum (500 MHz, 298 K, $\text{CDCl}_3:\text{CD}_3\text{CN} = 1:1$, 2.0 mM) of (a) the 1:1 mixture of **D10D** $^{2+}$ and **2a** and (b) the 1:2 mixture of **D10D** $^{2+}$ and **2a**. In figure (a), $K_1 = [0.16 \times 2.0 \times 10^{-3}] / [0.3 \times 2.0 \times 10^{-3}] / [2.0 \times 10^{-3} - 0.16 \times 2.0 \times 10^{-3} - 0.54 \times 2.0 \times 10^{-3} / 2] \text{ M}^{-1} = 468 \text{ M}^{-1}$; $K_2 = [0.54 \times 2.0 \times 10^{-3} / 2] / [0.16 \times 2.0 \times 10^{-3}] / [0.3 \times 2.0 \times 10^{-3}] \text{ M}^{-1} = 2813 \text{ M}^{-1}$; In figure (b), $K_1 = [0.08 \times 4.0 \times 10^{-3}] / [0.33 \times 4.0 \times 10^{-3}] / [2.0 \times 10^{-3} - 0.08 \times 4.0 \times 10^{-3} - 0.59 \times 4.0 \times 10^{-3} / 2] \text{ M}^{-1} = 485 \text{ M}^{-1}$; $K_2 = [0.59 \times 4.0 \times 10^{-3} / 2] / [0.08 \times 4.0 \times 10^{-3}] / [0.33 \times 4.0 \times 10^{-3}] \text{ M}^{-1} = 2794 \text{ M}^{-1}$; Finally, $K_1 = (468 + 485) / 2 = 476 (\pm 12) \text{ M}^{-1}$, $K_2 = (2813 + 2794) / 2 = 2803 (\pm 13) \text{ M}^{-1}$, $\alpha = 4K_2 / K_1 = 4 \times 2803 / 476 = 24$.

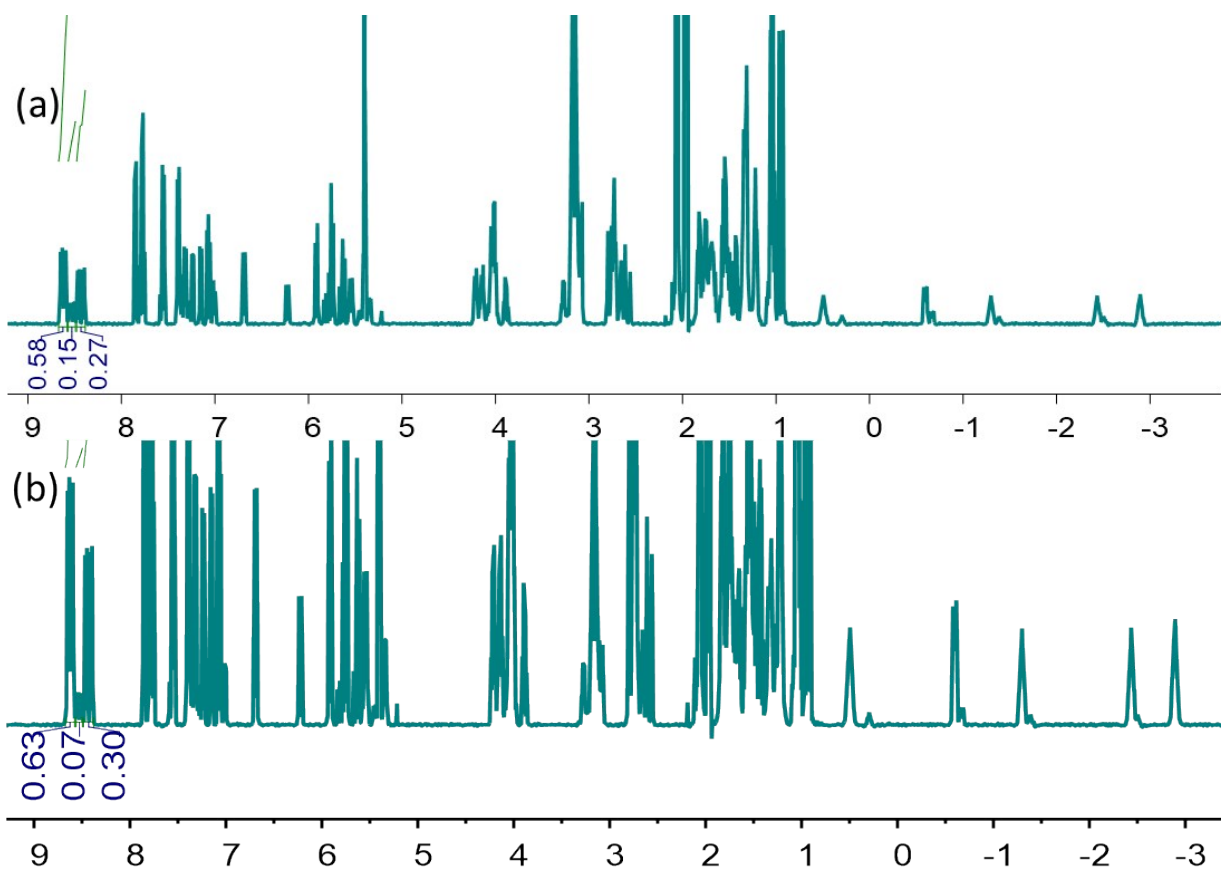


Fig. S23 ^1H NMR spectrum (500 MHz, 298 K, $\text{CDCl}_3:\text{CD}_3\text{CN} = 1:1$, 2.0 mM) of (a) the 1:1 mixture of **D11D** $^{2+}$ and **2a** and (b) the 1:2 mixture of **D11D** $^{2+}$ and **2a**. In figure (a), $K_1 = [0.15 \times 2.0 \times 10^{-3}] / [0.27 \times 2.0 \times 10^{-3}] / [(2.0 \times 10^{-3} - 0.15 \times 2.0 \times 10^{-3} - 0.58 \times 2.0 \times 10^{-3} / 2)] \text{ M}^{-1} = 496 \text{ M}^{-1}$; $K_2 = [0.58 \times 2.0 \times 10^{-3} / 2] / [0.15 \times 2.0 \times 10^{-3}] / [(0.27 \times 2.0 \times 10^{-3}) \text{ M}^{-1} = 3580 \text{ M}^{-1}$; In figure (b), $K_1 = [(0.08 / 1.01) \times 4.0 \times 10^{-3}] / [(0.30 / 1.01) \times 4.0 \times 10^{-3}] / [(2.0 \times 10^{-3} - (0.08 / 1.01) \times 4.0 \times 10^{-3} - (0.63 / 1.01) \times 4.0 \times 10^{-3} / 2)] \text{ M}^{-1} = 612 \text{ M}^{-1}$; $K_2 = [(0.63 / 1.01) \times 4.0 \times 10^{-3} / 2] / [(0.08 / 1.01) \times 4.0 \times 10^{-3}] / [(0.30 / 1.01) \times 4.0 \times 10^{-3}] \text{ M}^{-1} = 3750 \text{ M}^{-1}$; Finally, $K_1 = (496 + 507) / 2 = 502 (\pm 8) \text{ M}^{-1}$, $K_2 = (3580 + 3750) / 2 = 3665 (\pm 120) \text{ M}^{-1}$, $\alpha = 4K_2 / K_1 = 4 \times 3665 / 502 = 29$.

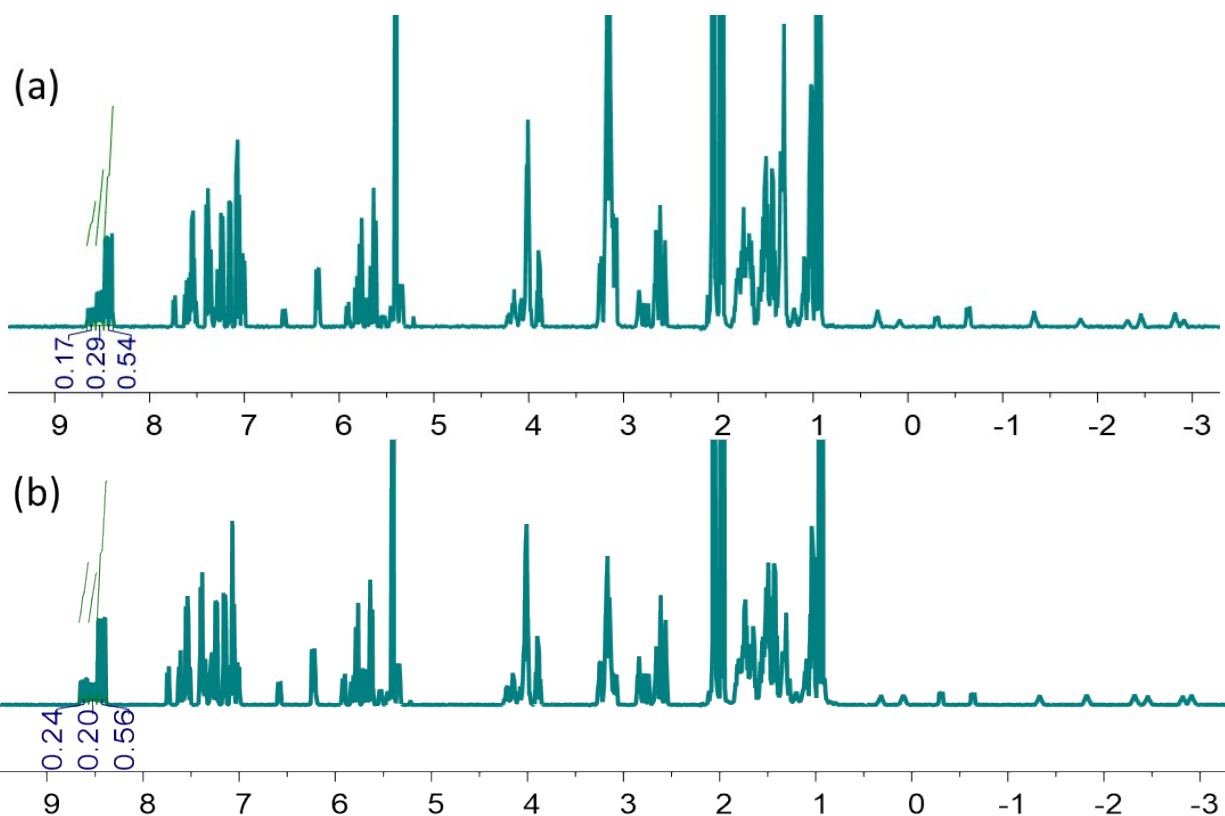


Fig. S24 ^1H NMR spectrum (500 MHz, 298 K, $\text{CDCl}_3:\text{CD}_3\text{CN} = 1:1$, 2.0 mM) of (a) the 1:1 mixture of D12D^{2+} and **2a** and (b) the 1:2 mixture of D12D^{2+} and **2a**. In figure (a), $K_1 = [0.29 \times 2.0 \times 10^{-3}] / [0.54 \times 2.0 \times 10^{-3}] / [2.0 \times 10^{-3} - 0.29 \times 2.0 \times 10^{-3} - 0.17 \times 2.0 \times 10^{-3} / 2] \text{ M}^{-1} = 430 \text{ M}^{-1}$; $K_2 = [0.17 \times 2.0 \times 10^{-3} / 2] / [0.29 \times 2.0 \times 10^{-3}] / [(0.54 \times 2.0 \times 10^{-3}) \text{ M}^{-1} = 271 \text{ M}^{-1}$; In figure (b), $K_1 = [0.20 \times 4.0 \times 10^{-3}] / [0.56 \times 4.0 \times 10^{-3}] / [2.0 \times 10^{-3} - 0.20 \times 4.0 \times 10^{-3} - 0.24 \times 4.0 \times 10^{-3} / 2] \text{ M}^{-1} = 496 \text{ M}^{-1}$; $K_2 = [0.24 \times 4.0 \times 10^{-3} / 2] / [0.20 \times 4.0 \times 10^{-3}] / [0.56 \times 4.0 \times 10^{-3}] \text{ M}^{-1} = 268 \text{ M}^{-1}$; Finally, $K_1 = (430 + 496) / 2 = 463 (\pm 46) \text{ M}^{-1}$, $K_2 = (271 + 268) / 2 = 270 (\pm 2) \text{ M}^{-1}$, $\alpha = 4K_2 / K_1 = 4 \times 270 / 463 = 2$.

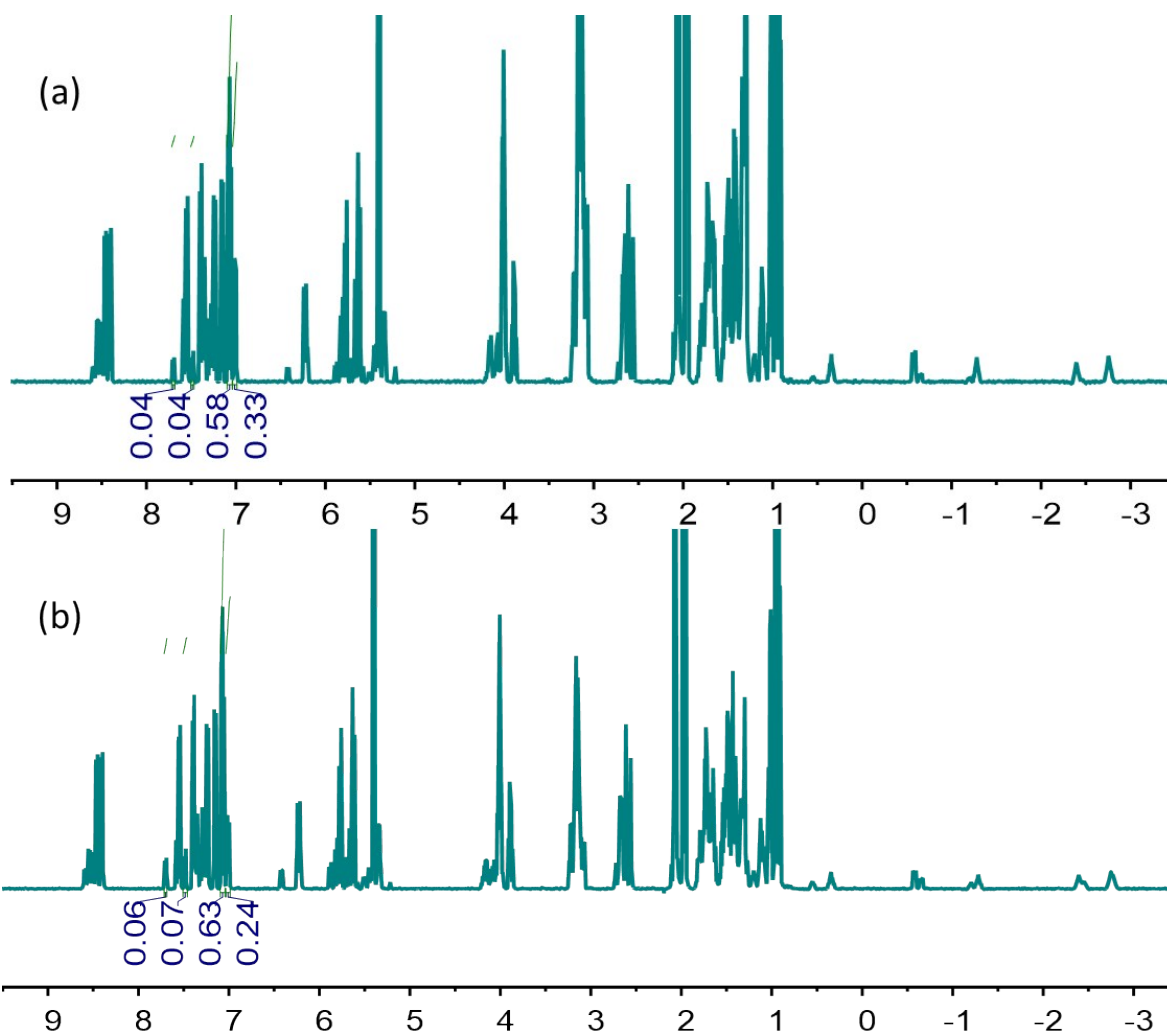


Fig. S25 ^1H NMR spectrum (500 MHz, 298 K, $\text{CDCl}_3:\text{CD}_3\text{CN} = 1:1$, 2.0 mM) of (a) the 1:1 mixture of **D13D** $^{2+}$ and **2a** and (b) the 1:2 mixture of **D13D** $^{2+}$ and **2a**. In figure (a), $K_1 = [0.33 \times 2.0 \times 10^{-3}] / [0.58 \times 2.0 \times 10^{-3}] / [2.0 \times 10^{-3} - 0.33 \times 2.0 \times 10^{-3} - 0.08 \times 2.0 \times 10^{-3} / 2] \text{ M}^{-1} = 452 \text{ M}^{-1}$; $K_2 = [0.08 \times 2.0 \times 10^{-3} / 2] / [0.33 \times 2.0 \times 10^{-3}] / [(0.58 \times 2.0 \times 10^{-3}) \text{ M}^{-1} = 104 \text{ M}^{-1}$; In figure (b), $K_1 = [0.24 \times 4.0 \times 10^{-3}] / [0.63 \times 4.0 \times 10^{-3}] / [2.0 \times 10^{-3} - 0.24 \times 4.0 \times 10^{-3} - 0.13 \times 4.0 \times 10^{-3} / 2] \text{ M}^{-1} = 421 \text{ M}^{-1}$; $K_2 = [0.13 \times 4.0 \times 10^{-3} / 2] / [0.24 \times 4.0 \times 10^{-3}] / [0.63 \times 4.0 \times 10^{-3}] \text{ M}^{-1} = 100 \text{ M}^{-1}$; Finally, $K_1 = (452 + 421) / 2 = 436 (\pm 22) \text{ M}^{-1}$, $K_2 = (104 + 100) / 2 = 102 (\pm 3) \text{ M}^{-1}$, $\alpha = 4K_2 / K_1 = 4 \times 102 / 436 = 0.9$.

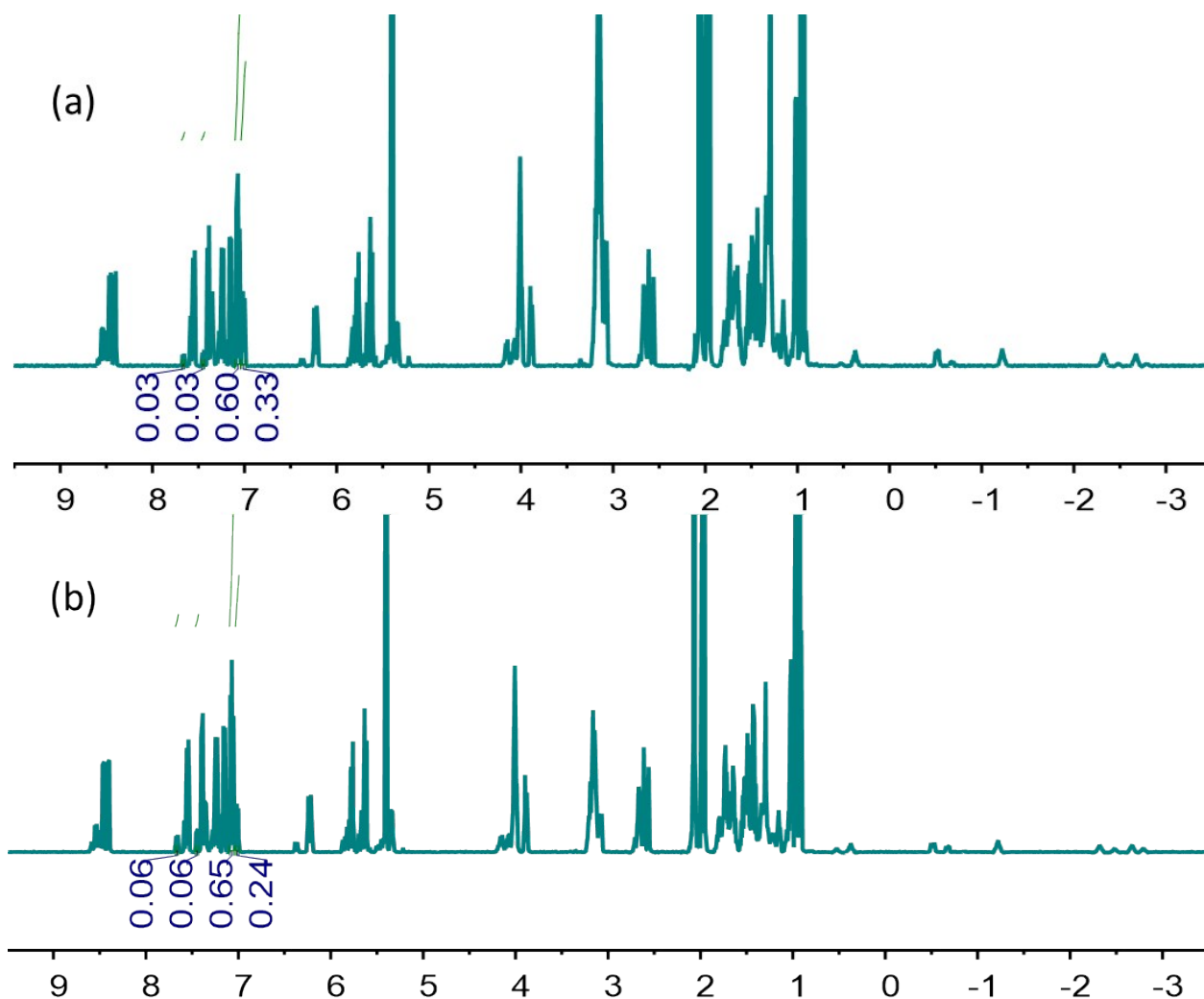


Fig. S26 ^1H NMR spectrum (500 MHz, 298 K, $\text{CDCl}_3:\text{CD}_3\text{CN} = 1:1$, 2.0 mM) of (a) the 1:1 mixture of D14D^{2+} and **2a** and (b) the 1:2 mixture of D14D^{2+} and **2a**. In figure (a), $K_1 = [0.33 \times 2.0 \times 10^{-3}] / [0.60 \times 2.0 \times 10^{-3}] / [2.0 \times 10^{-3} - 0.33 \times 2.0 \times 10^{-3} - 0.06 \times 2.0 \times 10^{-3} / 2] \text{ M}^{-1} = 430 \text{ M}^{-1}$; $K_2 = [0.06 \times 2.0 \times 10^{-3} / 2] / [0.33 \times 2.0 \times 10^{-3}] / [0.60 \times 2.0 \times 10^{-3}] \text{ M}^{-1} = 76 \text{ M}^{-1}$; In figure (b), $K_1 = [0.24 \times 4.0 \times 10^{-3}] / [0.65 \times 4.0 \times 10^{-3}] / [(2.0 \times 10^{-3} - 0.24 \times 4.0 \times 10^{-3} - 0.12 \times 4.0 \times 10^{-3} / 2) \text{ M}^{-1} = 462 \text{ M}^{-1}$; $K_2 = [0.12 \times 4.0 \times 10^{-3} / 2] / [0.24 \times 4.0 \times 10^{-3}] / [0.65 \times 4.0 \times 10^{-3}] \text{ M}^{-1} = 96 \text{ M}^{-1}$; Finally, $K_1 = (430 + 462) / 2 = 446 (\pm 23) \text{ M}^{-1}$, $K_2 = (76 + 96) / 2 = 86 (\pm 14) \text{ M}^{-1}$, $\alpha = 4K_2 / K_1 = 4 \times 86 / 446 = 0.8$.

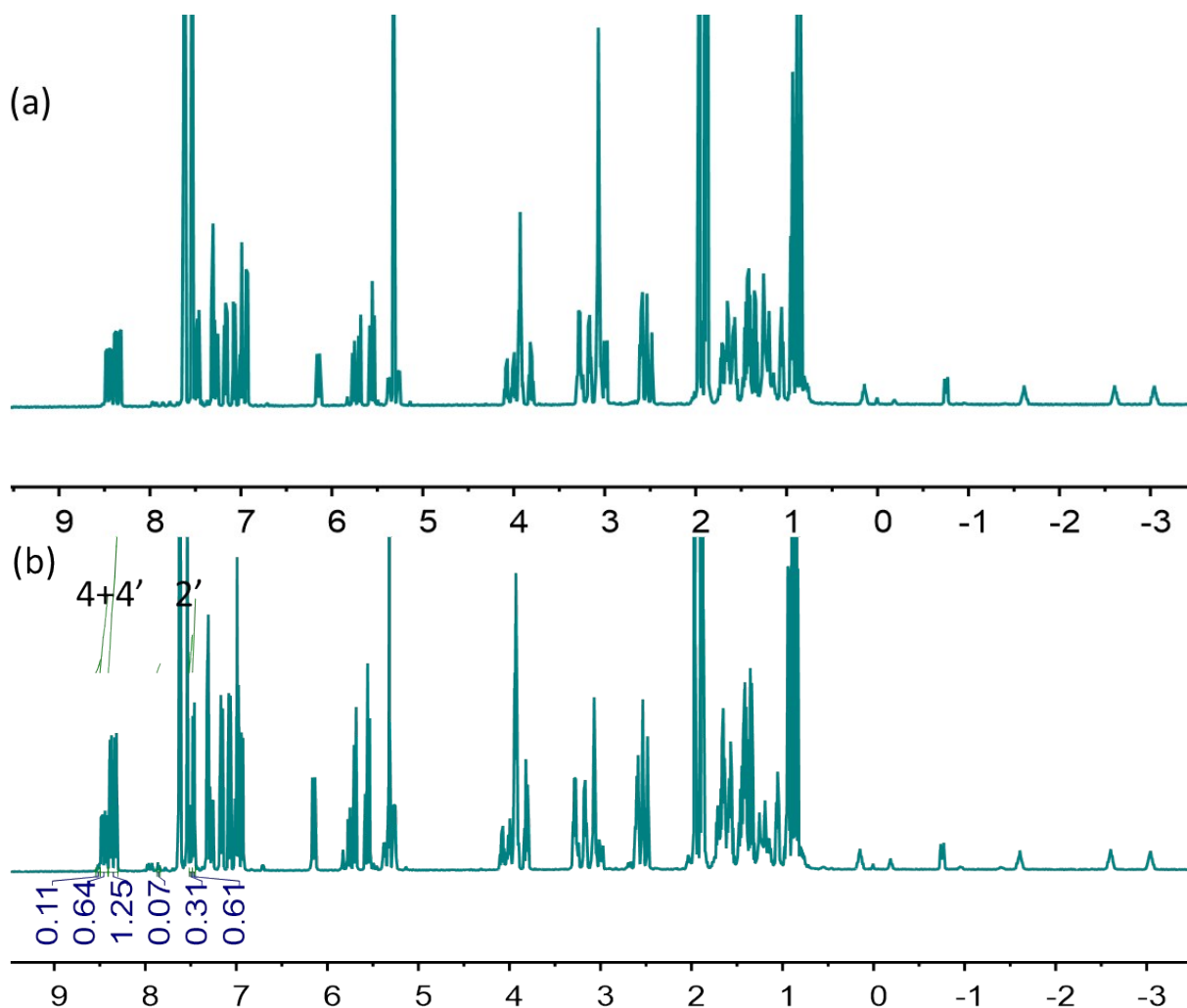


Fig. S27 ^1H NMR spectrum (500 MHz, 298 K, $\text{CDCl}_3:\text{CD}_3\text{CN} = 1:1$) of 2:1 mixture of **2a** with guest **D9D-2BArF** (2.0 mM). It is quite difficult to accurately determine the stepwise binding constants in 1:1 mixture of **D9D** $^{2+}$ and **2a** since the complex **D9D** $^{2+}@\mathbf{2a}_2$ only exist in very small amount. In figure (b), from complexed and uncomplexed $\text{H}_{4+4'}$ and $\text{H}_{2'}$ of **2a**, $K_1(\text{H}_{4+4'}) = [(0.64 / 2) \times 4.0 \times 10^{-3}] / [(1.25 / 2) \times 4.0 \times 10^{-3}] / [4.0 \times 10^{-3} - (0.64 / 2) \times 4.0 \times 10^{-3} - (0.11 / 2) \times 4.0 \times 10^{-3} / 2] \text{ M}^{-1} = 839 \text{ M}^{-1}$; $K_2(\text{H}_{4+4'}) = [(0.11 / 2) \times 4.0 \times 10^{-3} / 2] / [(0.64 / 2) \times 4.0 \times 10^{-3}] / [(0.64 / 2) \times 4.0 \times 10^{-3}] \text{ M}^{-1} = 34 \text{ M}^{-1}$; $K_1(\text{H}_{2'}) = [(0.31 / 0.99) \times 4.0 \times 10^{-3}] / [(0.61 / 0.99) \times 4.0 \times 10^{-3}] / [(4.0 \times 10^{-3} - (0.31 / 0.99) \times 4.0 \times 10^{-3} - (0.07 / 0.99) \times 4.0 \times 10^{-3} / 2] \text{ M}^{-1} = 820 \text{ M}^{-1}$; $K_2(\text{H}_{2'}) = [(0.07 / 0.99) \times 4.0 \times 10^{-3} / 2] / [(0.31 / 0.99) \times 4.0 \times 10^{-3}] / [(0.61 / 0.99) \times 4.0 \times 10^{-3}] \text{ M}^{-1} = 46 \text{ M}^{-1}$; Finally, $K_1 = (839 + 820) / 2 = 830 (\pm 13) \text{ M}^{-1}$, $K_2 = (34 + 46) / 2 = 40 (\pm 8) \text{ M}^{-1}$, $\alpha = 4K_2 / K_1 = 4 \times 40 / 830 = 0.2$.

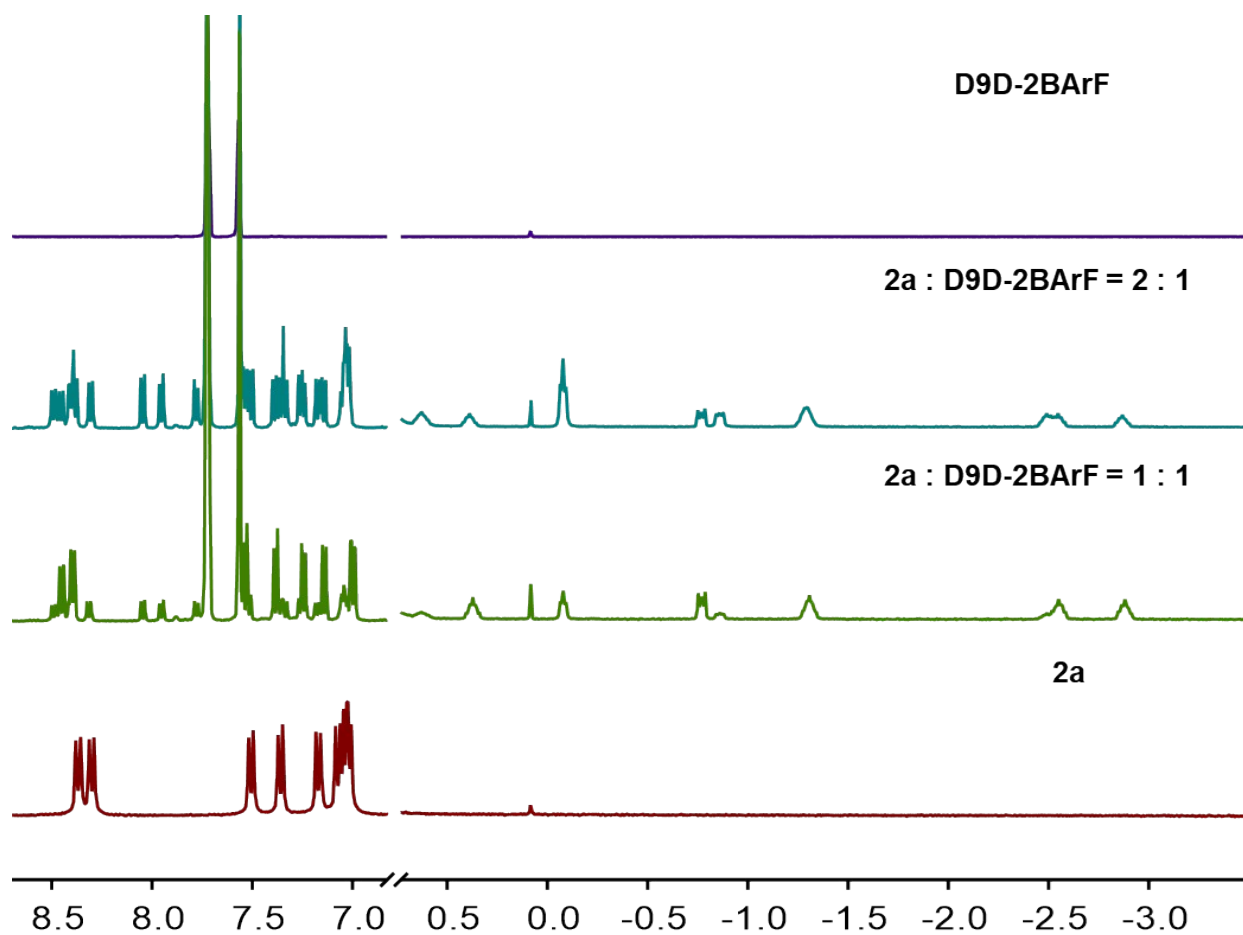


Fig. S28 Partial ^1H NMR spectra (500 MHz, CD_2Cl_2 , 298 K) of **2a** and 1:1 and 2:1 mixture of **2a** with guest **D9D-2BArF** (2.0 mM). The counterion is BArF^- , **D9D** $^{2+}$ can undergo stepwise binding with two **2a**.

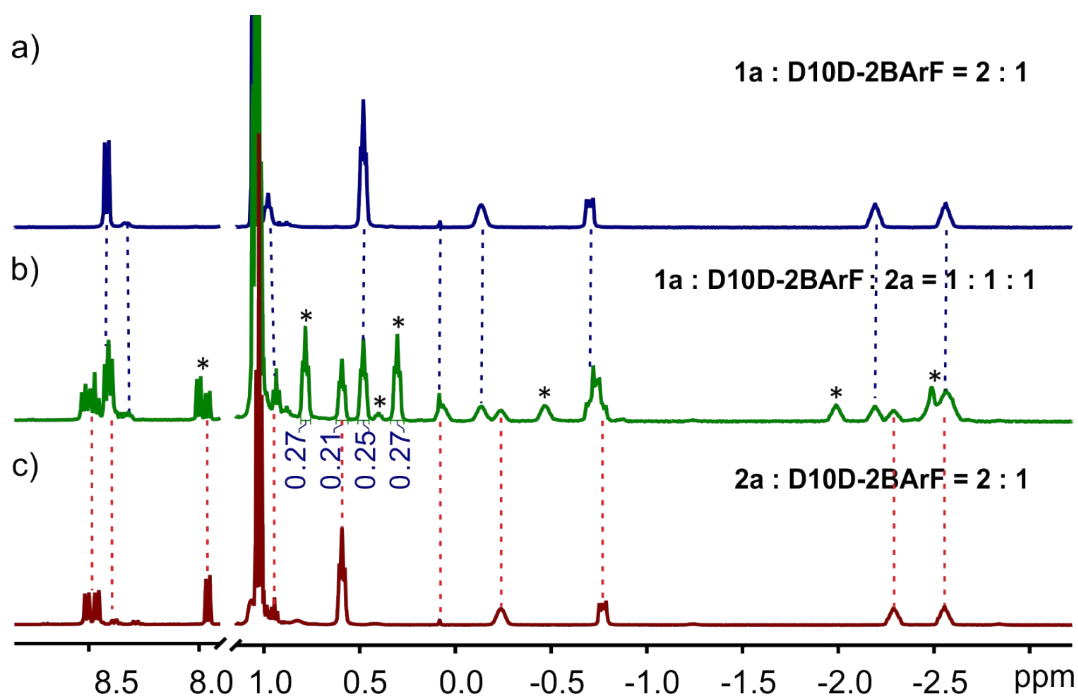


Fig. S29 Selected region of ^1H NMR spectra (500 MHz, CD_2Cl_2 , 2.0 mM, 298 K) of (a) 2:1 mixture of **1a** with **D10D-2BArF**; (b) the equimolar mixture of **1a**, **D10D-2BArF**, and **2a**; (c) 2:1 mixture of **2a** with **D10D-2BArF**. In the equimolar mixture of **1a**, **2a** and **D9D-2BArF**, a set of new peaks was detected besides the peaks of $\mathbf{1a}_2@D10D^{2+}$ and $\mathbf{2a}_2@D10D^{2+}$, indicated the formation of another complex. “*” indicated the new complex.

Diffusion ordered NMR spectroscopy (DOSY). A LED29 pulse sequence (ledbpgp2s) was used for the diffusion experiments with a sine-shape pulsed gradient duration δ (P30) of 800 ms incremented from 0.68 to 32.4 G cm⁻¹ in 16 steps. The pulsed gradient separation Δ (D20) was 200 ms, the spoil gradient (P19) was set to 600 μ s, and the eddy current delay (D21) was 5 ms. The reported diffusion coefficients were obtained using the T1/T2 relaxation module in TopSpin 3.2 software.

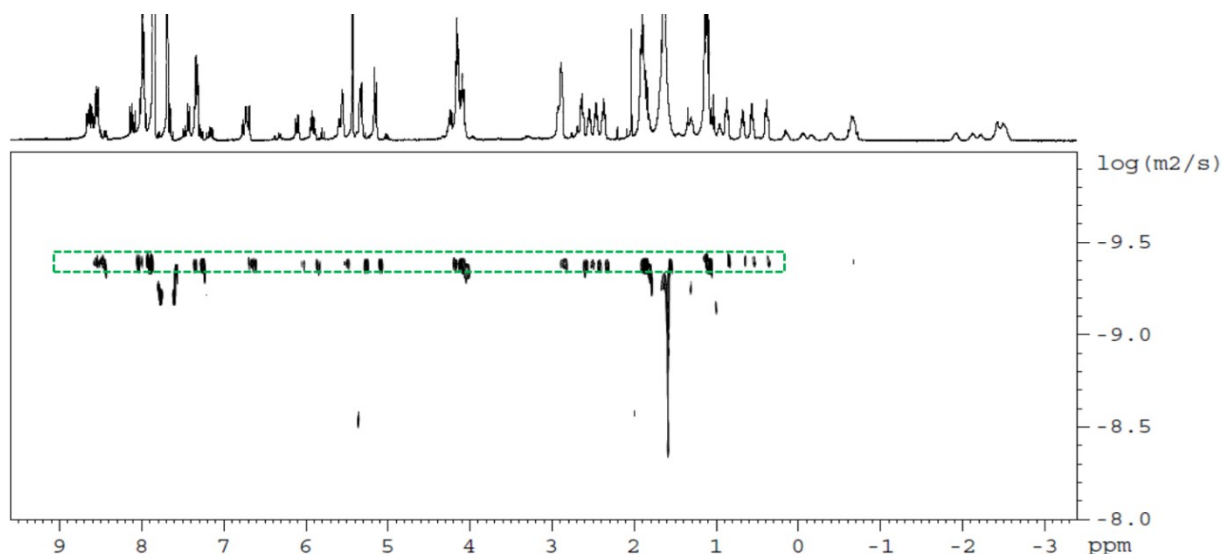


Fig. S30 DOSY NMR spectrum (400 MHz, CD₂Cl₂, 298 K) showing the very similar diffusion behavior of the complex **D10D-2BArF@1a.2a**, **D10D-2BArF@1a₂** and **D10D-2BArF@2a₂**. The diffusion coefficient for the three complexes **D10D-2BArF@1a.2a**, **D10D-2BArF@1a₂** and **D10D-2BArF@2a₂** was calculated to be 3.94×10^{-10} m²s⁻¹, 3.91×10^{-10} m²s⁻¹, and 3.96×10^{-10} m²s⁻¹ respectively.

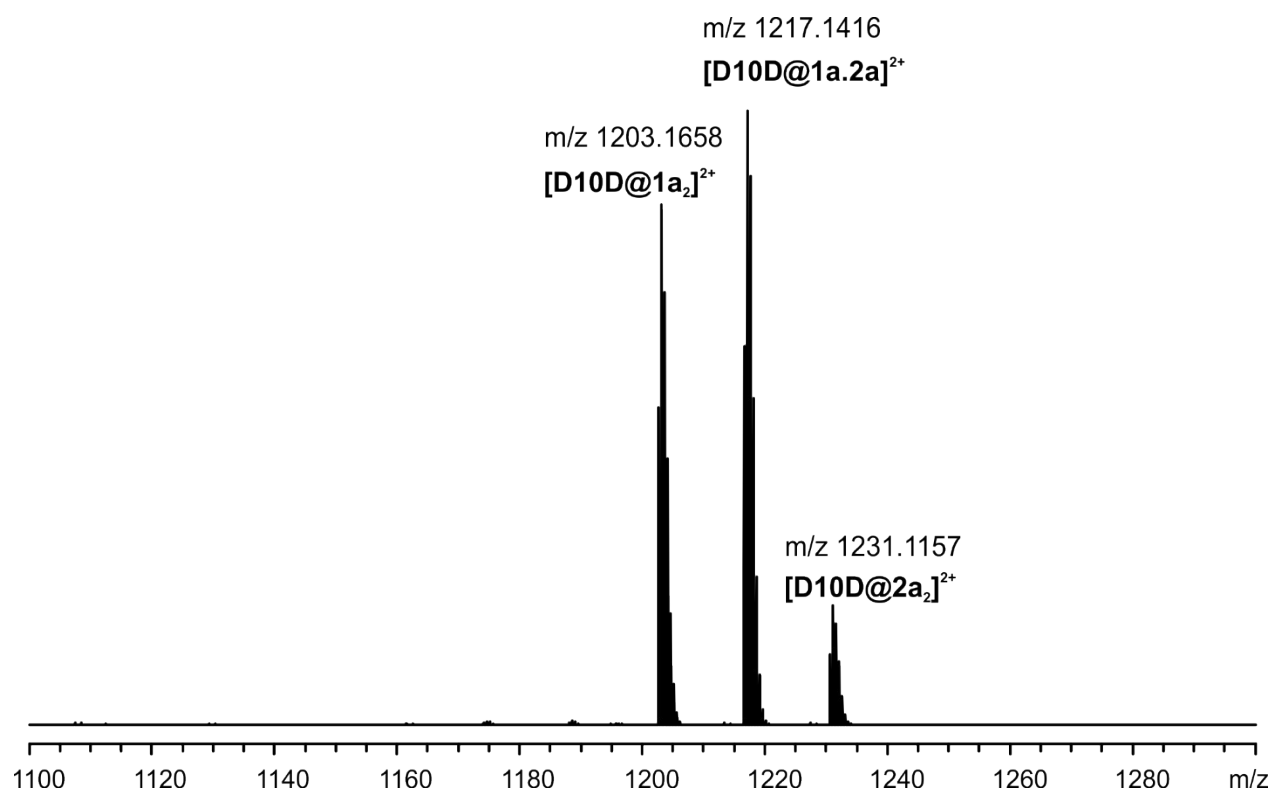


Fig. S31 ESI mass spectrum of the equimolar mixture of **1a**, **D10D-2BArF**, and **2a**.

3. Single Crystal X-Ray Crystallography

Suitable single crystals of **2a** and **2b** for structural determination were obtained by slow evaporation of the CH₂Cl₂ solution of **2a** and **2b**.

Single crystal X-ray data for **2a** and **2b** were collected with Agilent Super-Nova dual wavelength diffractometer with a micro-focus X-ray source and multilayer optics monochromatized Cu-K α ($\lambda = 1.54178 \text{ \AA}$) radiation. Program *CrysAlisPro*¹ was used for the data collection and reduction. The intensities were corrected for absorption using multi-scan absorption correction method² for all the data. The structures were solved with direct methods (*SHELXT*³) and refined by full-matrix least squares on F^2 using *SHELXL-2017* program.⁴ Anisotropic displacement parameters were assigned to non-H atoms. All hydrogen atoms were refined using riding models.

Crystal data and the structure refinements are summarized in **Table S1**. These crystal structures have been deposited in the Cambridge Crystallographic Data Centre (CCCD NO. are found in **Table S1**). These data can be obtained free of charge *via* www.ccdc.cam.ac.uk/data_request/cif, or by emailing data_request@ccdc.cam.ac.uk, or by contacting The Cambridge Crystallographic Data Centre, 12, Union Road, Cambridge CB2 1EZ, UK; fax: +44 1223 336033.

Table S1. Crystal data and structure refinement for **2a** and **2b**.

entry	2a	2b
Moiety formula	C ₆₆ H ₆₄ O ₁₂ ·(CH ₂ Cl ₂)	C ₆₆ H ₆₄ O ₁₂
Empirical formula	C ₆₇ H ₆₆ Cl ₂ O ₁₂	C ₆₆ H ₆₄ O ₁₂
Formula weight	1134.09	1049.17
Temperature/K	200	100
Crystal system	triclinic	triclinic
Space group	<i>P</i> -1	<i>P</i> -1
<i>a</i> /Å	12.3158(4)	9.3274(4)
<i>b</i> /Å	12.7690(4)	12.0859(5)
<i>c</i> /Å	19.5858(6)	12.407(5)
α /°	85.884(2)	110.921(2)
β /°	73.714(2)	90.774(2)
γ /°	80.961(2)	98.445(3)
Volume/Å ³	2918.52(16)	1290.40(9)
<i>Z</i>	2	1
ρ_{calc} /cm ³	1.291	1.350
μ /mm ⁻¹	1.521	0.746
F(000)	1196	556
Reflections collected	22961	12607
Independent reflections	8339 [R _{int} = 0.0397, R _{sigma} = 0.0474]	3701 [R _{int} = 0.0346, R _{sigma} = 0.0355]
Data/restraints/parameters	8339/1/757	3701/14/380
Goodness-of-fit on F ²	1.023	1.045
Final R indexes [I>>=2 σ (I)]	R ₁ = 0.0643, wR ₂ = 0.1889	R ₁ = 0.0408, wR ₂ = 0.0934

Final R indexes [all data]	R ₁ = 0.1085, wR ₂ = 0.2367	R ₁ = 0.0555, wR ₂ = 0.1019
CCDC number	1844454	1844453

2a

THETM01_ALERT_3_B The value of $\sin(\theta_{\max})/\lambda$ is less than 0.575

Calculated $\sin(\theta_{\max})/\lambda = 0.5555$

Response: The crystal has too weak diffraction to obtain high resolution data.

PLAT420_ALERT_2_B D-H Without Acceptor O5A --H18A . Please Check

PLAT420_ALERT_2_B D-H Without Acceptor O5B --H19A . Please Check

PLAT420_ALERT_2_B D-H Without Acceptor O7B --H35B . Please Check

Response: Carbonyl O5A, O7A (the second site of O5B, O7B) is on the ester group which is disordered although low temperature was used for the data collection.

2b

THETM01_ALERT_3_B The value of $\sin(\theta_{\max})/\lambda$ is less than 0.575

Calculated $\sin(\theta_{\max})/\lambda = 0.5565$

Response: The crystal has too weak diffraction to obtain high resolution data.

PLAT420_ALERT_2_B D-H Without Acceptor O5A --H18B . Please Check

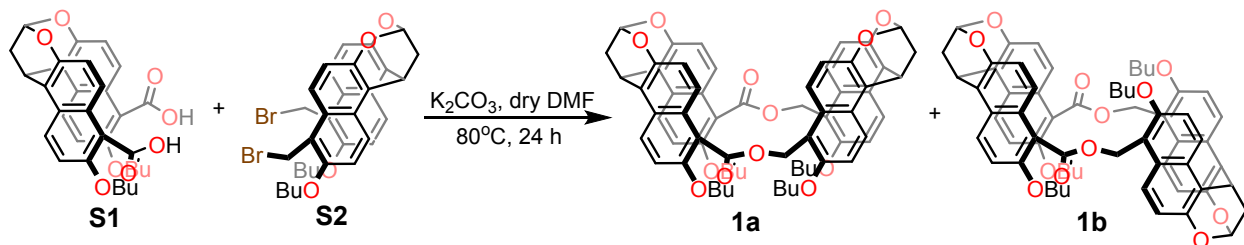
PLAT420_ALERT_2_B D-H Without Acceptor O5B --H19B . Please Check

Response: Carbonyl O5A (the second site of O5B) is on the ester group which is disordered although low temperature was used for the data collection.

4. Experimental Section

4.1 General Method. All the reagents involved in this research were commercially available and used without further purification unless otherwise noted. Solvents were either employed as purchased or dried prior to use by standard laboratory procedures. Thin-layer chromatography (TLC) was carried out on 0.25 mm Yantai silica gel plates (60F-254). Column chromatography was performed on silica gel 60 (Tsingdao40 – 63 nm, 230 – 400 mesh). ^1H , ^{13}C , ^1H - ^1H COSY, ^1H - ^1H ROESY, and DOSY NMR spectra were recorded on Bruker Avance-400 or 500 spectrometers. All chemical shifts are reported in *ppm* with residual solvents or TMS (tetramethylsilane) as the internal standards. The following abbreviations were used for signal multiplicities: s, singlet; d, doublet; t triplet; m, multiplet. Electrospray-ionization time-of-high-resolution mass spectra (ESI-HRMS) were recorded on a Bruker Apex IV FTMS mass spectrometer. All the computations were performed at the AM1 level of theory by using Spartan'14 (Wavefunction, Inc.). The synthesis of guests **D2D**²⁺ - **D8D**²⁺,⁵ **D10D**²⁺ and **D12D**²⁺,⁶ **D9D**²⁺ and **D11D**²⁺ - **D14D**²⁺,⁷ and compounds **S1**⁸ and **S2**⁷ has been reported.

4.2 Synthetic Route of 2a and 2b

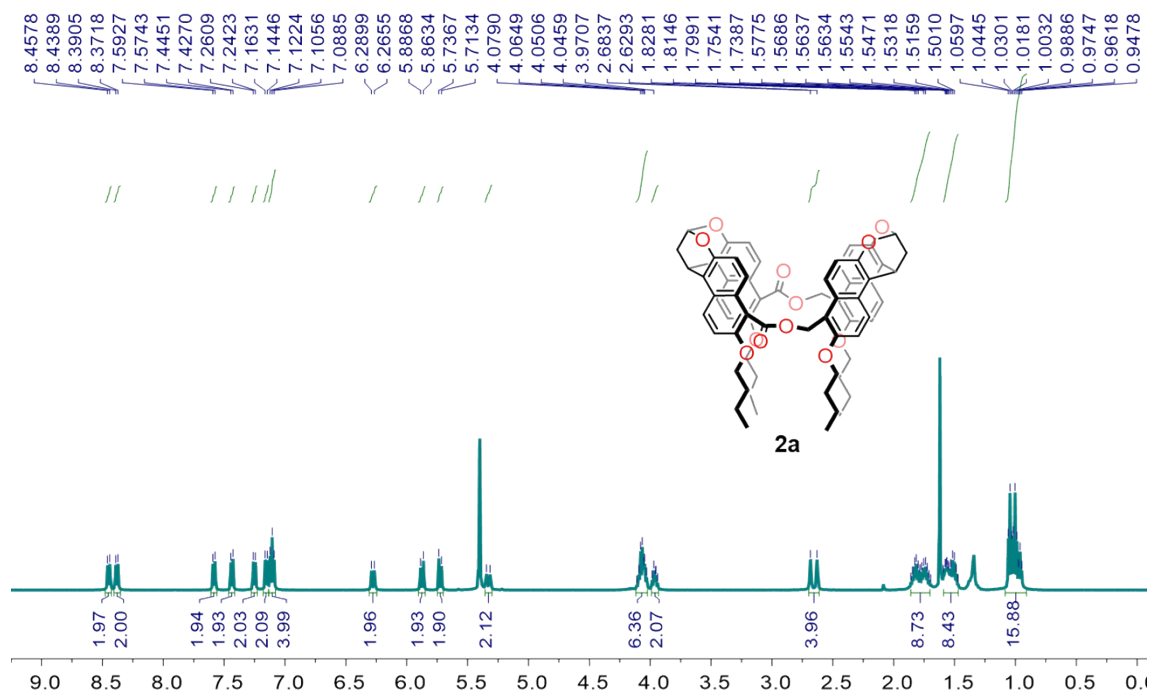


Compound 2a and 2b

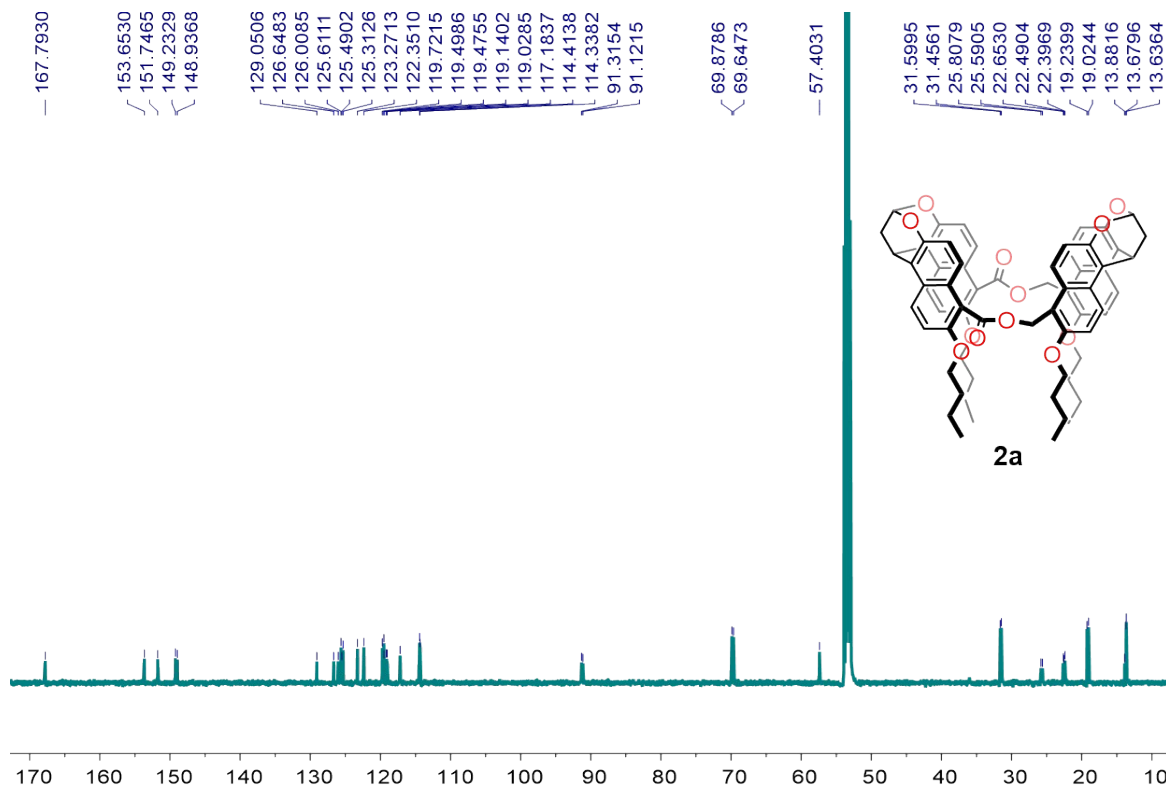
Potassium carbonate (500 mg, 35.9 mmol) and 500 mL dry DMF were added into a 1000-mL three-neck flask charged with a magnetic stirring bar. The flask was then evacuated and refilled with Ar (using a gas balloon). The solution of **S1** (250 mg, 4.5 mmol, in 60 mL dry DMF) and **S2** (294 mg, 4.5 mmol, in 60 mL dry DMF) were added dropwise using two separate syringes to the flask *via* a double-channel syringe pump during 10 h. Then the reaction mixture was stirred for another 24 h at 80 °C. After removing most of the solvent in vacuum, the residue was poured into 1.0 M HCl (200 mL). The precipitate was then filtered and washed with water extensively to give an off-white solid, which was purified by column chromatography (SiO_2 , CH_2Cl_2 : Hexane = 1:1

~ 2:1) to afford pure products **2a** (510 mg, yield 11 %) and **2b** (750 mg, yield 16 %) as white solids.

2a. m.p. > 300 °C; ¹H NMR (500 MHz, CD₂Cl₂, 298K) δ [ppm] = 8.45 (d, *J* = 9.4 Hz, 2H), 8.38 (d, *J* = 9.4 Hz, 2H), 7.58 (d, *J* = 9.2 Hz, 2H), 7.44 (d, *J* = 9.1 Hz, 2H), 7.25 (d, *J* = 9.3 Hz, 2H), 7.15 (d, *J* = 9.3 Hz, 2H), 7.11 (t, *J* = 8.5 Hz, 4H), 6.28 (d, *J* = 12.2 Hz, 2H), 5.88 (d, *J* = 11.7 Hz, 2H), 5.73 (d, *J* = 11.7 Hz, 2H), 5.33 (d, *J* = 15.0 Hz, 2H), 4.12 - 4.02 (m, 6H), 3.99 - 3.93 (m, 2H), 2.66 (d, *J* = 27.2 Hz, 4H), 1.86 - 1.71 (m, 8H), 1.59 - 1.47 (m, 8H), 1.06 - 0.95 (m, *J* = 20.4, 7.3 Hz, 12H); ¹³C NMR (125 MHz, CD₂Cl₂, 298K) δ [ppm] = 167.8, 153.7, 151.8, 149.2, 148.9, 129.1, 126.7, 126.0, 125.6, 125.5, 125.3, 123.3, 122.4, 119.7, 119.5, 119.5, 119.1, 119.0, 117.2, 114.4, 114.3, 91.3, 91.1, 69.9, 69.7, 57.4, 31.6, 31.5, 25.8, 25.6, 22.7, 22.5, 22.4, 19.2, 19.0, 13.9, 13.7, 13.6; HRMS (ESI): *m/z* calcd for [M+NH₄]⁺ C₆₆H₆₈O₁₂N⁺, 1066.4736; found 1066.4761 (error = -0.4 ppm); calcd for [M+H]⁺ C₆₆H₆₅O₁₂⁺, 1049.4471; found 1049.4473 (error = -0.2 ppm).

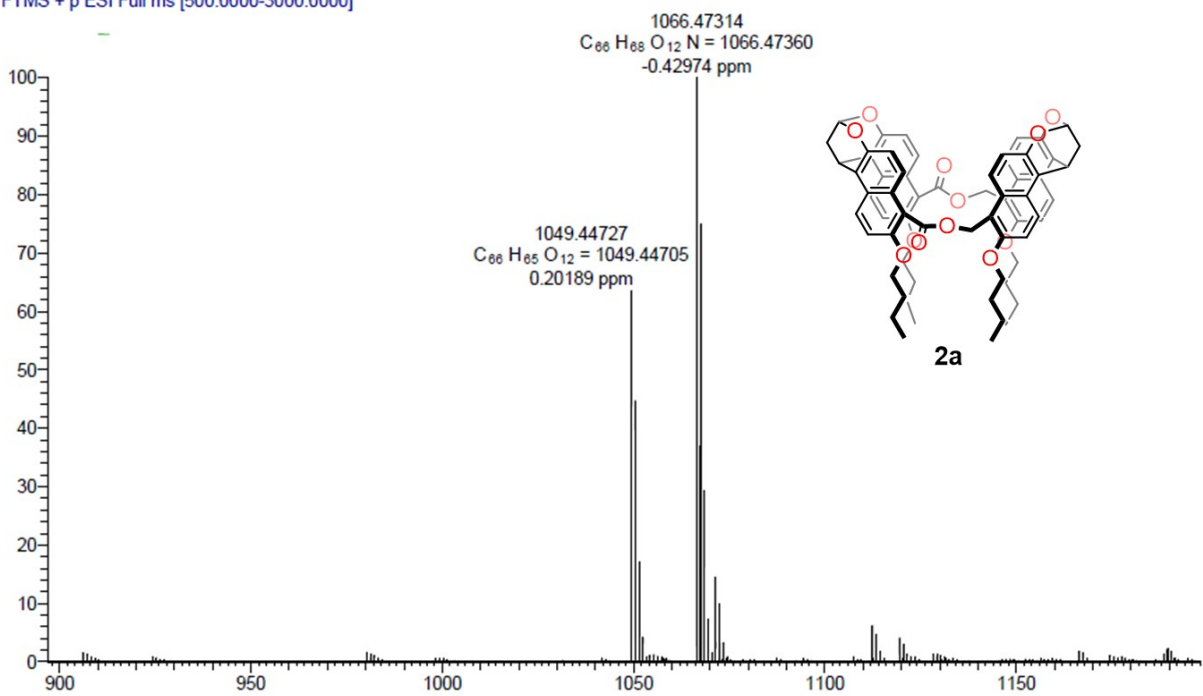


¹H NMR spectrum (500 MHz, CD₂Cl₂, 298 K) of compound **2a**



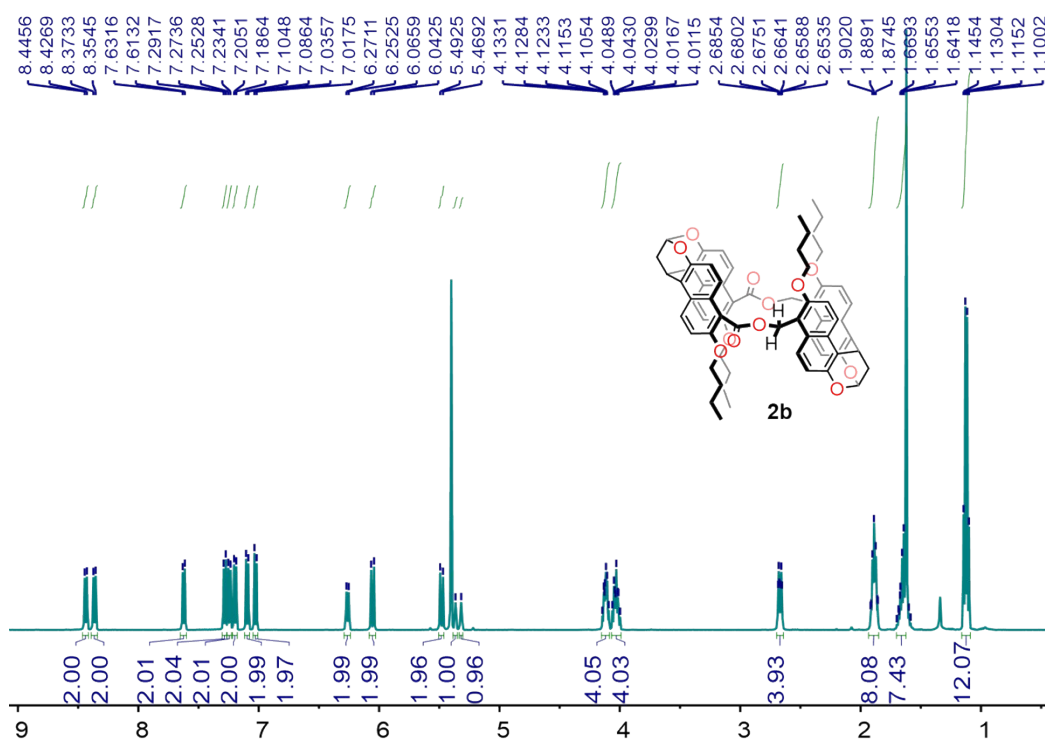
^{13}C NMR spectrum (125 MHz, CD_2Cl_2 , 298 K) of compound **2a**

chx-m2#15 RT: 0.22 AV: 1 NL: 6.81E7
T: FTMS + p ESI Full ms [500.0000-3000.0000]

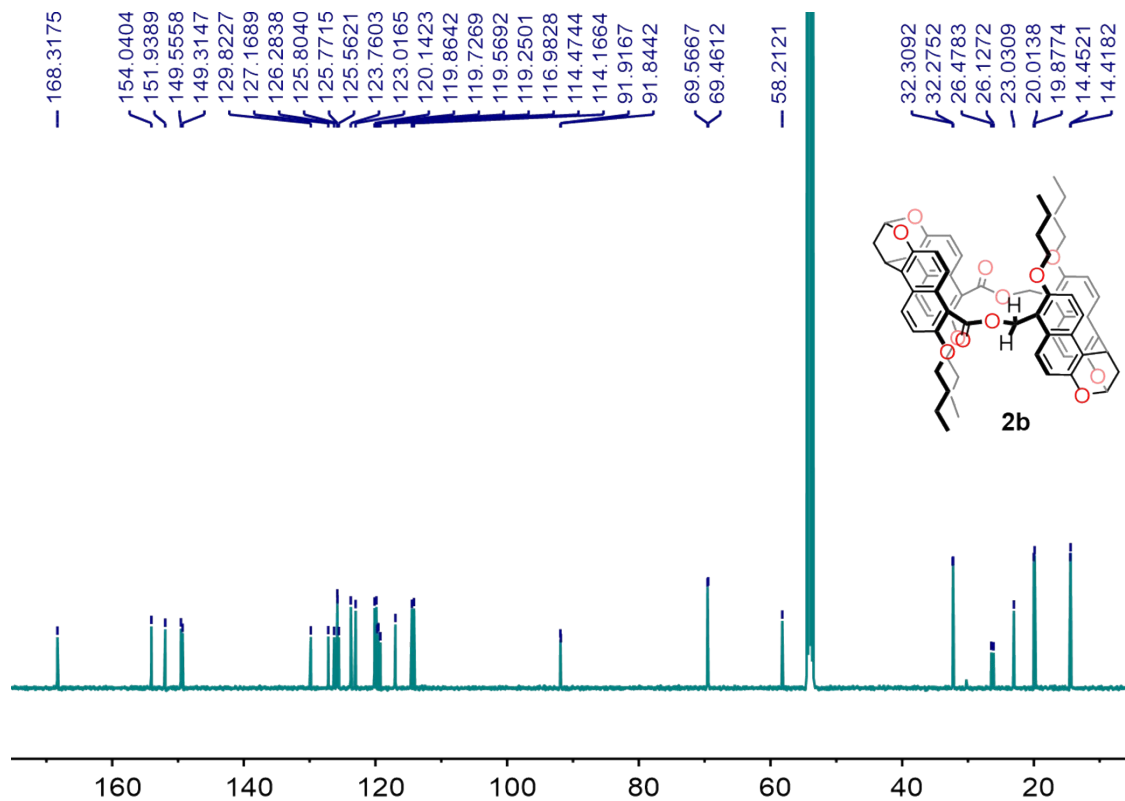


ESI mass spectrum of compound **2a**

2b. m.p. > 300 °C; ^1H NMR (500 MHz, CD_2Cl_2 , 298 K) δ [ppm] = 8.44 (d, $J = 9.4$ Hz, 2H), 8.36 (d, $J = 9.4$ Hz, 2H), 7.62 (d, $J = 9.2$ Hz, 2H), 7.28 (d, $J = 9.1$ Hz, 2H), 7.24 (d, $J = 9.4$ Hz, 2H), 7.20 (d, $J = 9.4$ Hz, 2H), 7.10 (d, $J = 9.2$ Hz, 2H), 7.03 (d, $J = 9.1$ Hz, 2H), 6.26 (d, $J = 9.3$ Hz, 2H), 6.05 (d, $J = 11.7$ Hz, 2H), 5.48 (d, $J = 11.7$ Hz, 2H), 5.37 (s, 1H), 5.32 (s, 1H), 4.15 - 4.09 (m, 4H), 4.06 - 4.00 (m, 4H), 2.67 (dt, $J = 10.8, 2.6$ Hz, 4H), 1.93 - 1.85 (m, 8H), 1.70 - 1.58 (m, 8H), 1.12 (q, $J = 7.5$ Hz, 12H); ^{13}C NMR (125 MHz, CD_2Cl_2) δ [ppm] = 168.3, 154.0, 151.9, 149.6, 149.3, 129.8, 127.2, 126.3, 125.8, 125.8, 125.6, 123.8, 123.0, 120.1, 119.9, 119.7, 119.6, 119.3, 117.0, 114.5, 114.2, 91.9, 91.8, 69.6, 69.5, 58.2, 32.3, 32.3, 26.5, 26.1, 23.0, 20.0, 19.9, 14.5, 14.4; HRMS (ESI): m/z calcd for $[\text{M}+\text{H}]^+ \text{C}_{66}\text{H}_{65}\text{O}_{12}^+$, 1049.4471; found 1049.4501 (error = 3.3 ppm); calcd for $[\text{M}+\text{Na}]^+ \text{C}_{66}\text{H}_{64}\text{O}_{12}\text{Na}^+$, 1071.4290; found 1071.4309 (error = 1.8 ppm).

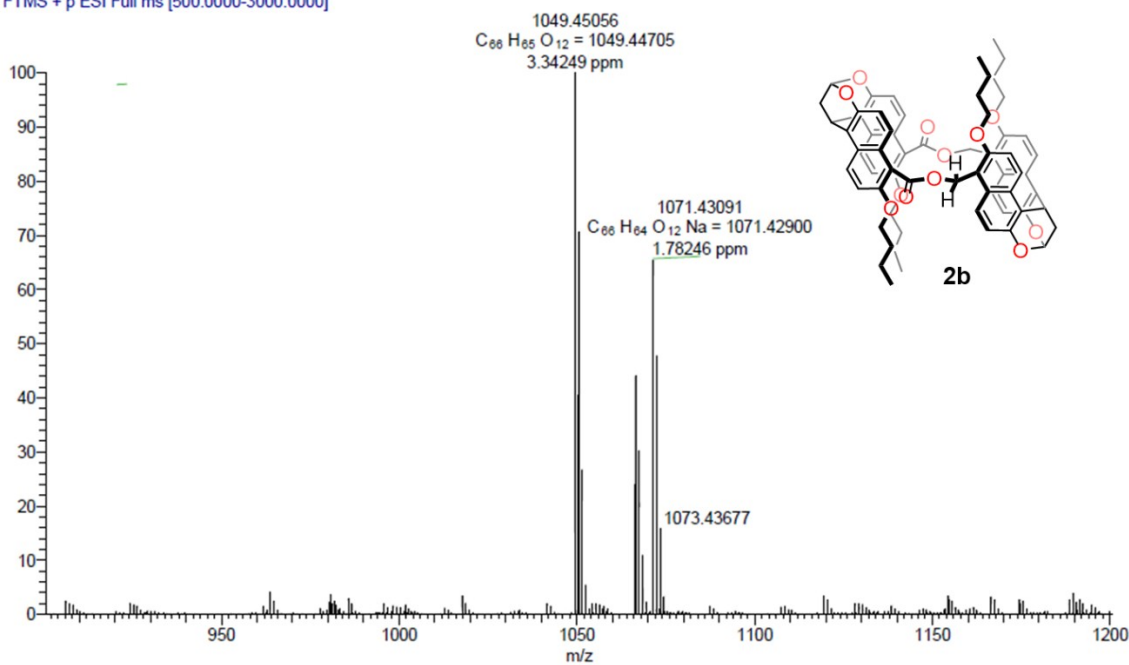


^1H NMR spectrum (500 MHz, CD_2Cl_2 , 298 K) of compound **2b**



¹³C NMR spectrum (125 MHz, CD₂Cl₂, 298 K) of compound **2b**

chx-m1 171208142732 #29 RT: 0.45 AV: 1 NL: 4.93E6
T: FTMS + p ESI Full ms [500.0000-3000.0000]

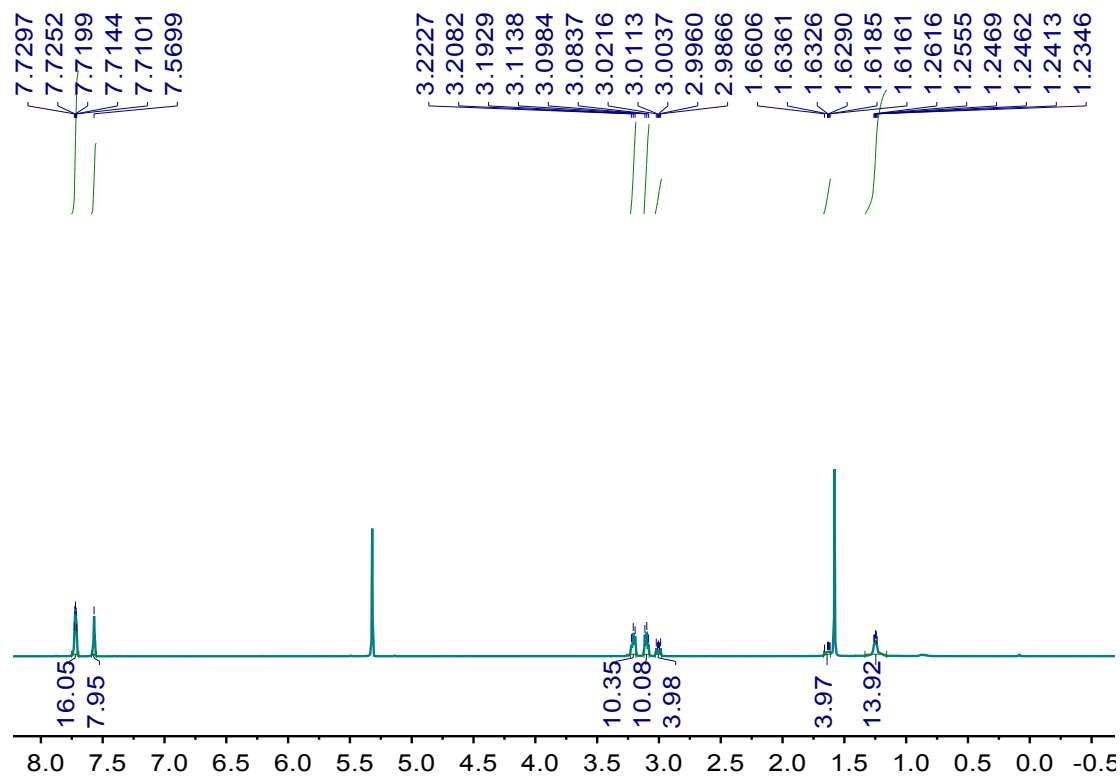


ESI mass spectrum of compound **2b**

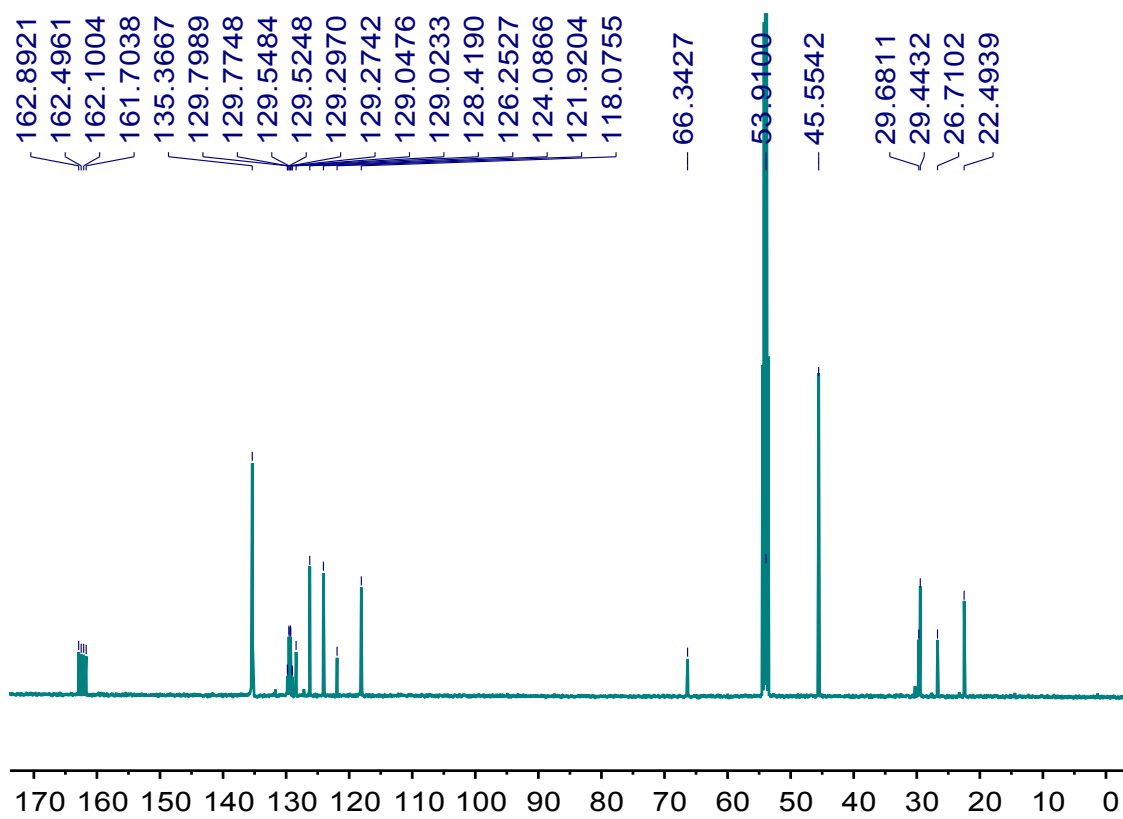
4.3 Synthesis of Guests **D9D-2BArF** & **D10D-2BArF**

Organic cationic guests **D9D**²⁺ and **D10D**²⁺ with BArF⁻ as counterions were prepared from their bromide salts⁵ by following the literature procedure.⁹

D9D-2BArF: NaBArF (500 mg, 0.6 mmol) was dissolved in methanol (20 mL). The solution of **D9D-2Br** (127 mg, 0.25 mmol) in methanol (10 mL) was added dropwise into the saturated solution of NaBArF. The resulting mixture was stirred vigorously overnight. Then the solvent was removed in vacuum. The residue was suspended in H₂O (20 mL), extracted with CH₂Cl₂ (20 mL × 3). The organic layer was collected, washed with H₂O (50 mL), dried with Na₂SO₄. The solvent was then evaporated in vacuum to afford **D9D-2BArF** as a white solid (490 mg, 95 %). m.p. 152-153 °C; ¹H NMR (500 MHz, CD₂Cl₂, 298 K) δ [ppm] = 7.72-7.71 (m, 16H), 7.57 (s, 8H), 3.21 (t, *J* = 7.4 Hz, 10H), 3.10 (t, *J* = 7.5 Hz, 10H), 3.03 - 2.98 (m, 4H), 1.67 - 1.61 (m, 4H), 1.33 - 1.16 (m, 14H); ¹³C NMR (125 MHz, CD₂Cl₂, 298 K) δ [ppm] = 162.3 (q, ¹*J*_{CB} = 50 Hz), 135.4, 129.4 (q, ²*J*_{CF} = 50 Hz), 125.2 (q, ¹*J*_{CF} = 270 Hz), 118.1, 66.4, 53.9, 45.6, 29.7, 29.4, 26.7, 22.5; HRMS (ESI): *m/z* calcd for [M-2BArF]²⁺ C₂₁H₄₂N₄²⁺, 175.1699; found 175.1699 (error = -0.1 ppm); calcd for [BArF]⁻ C₃₂H₁₂BF₂₄⁻, 863.0654; found 863.0649 (error = -0.6 ppm).



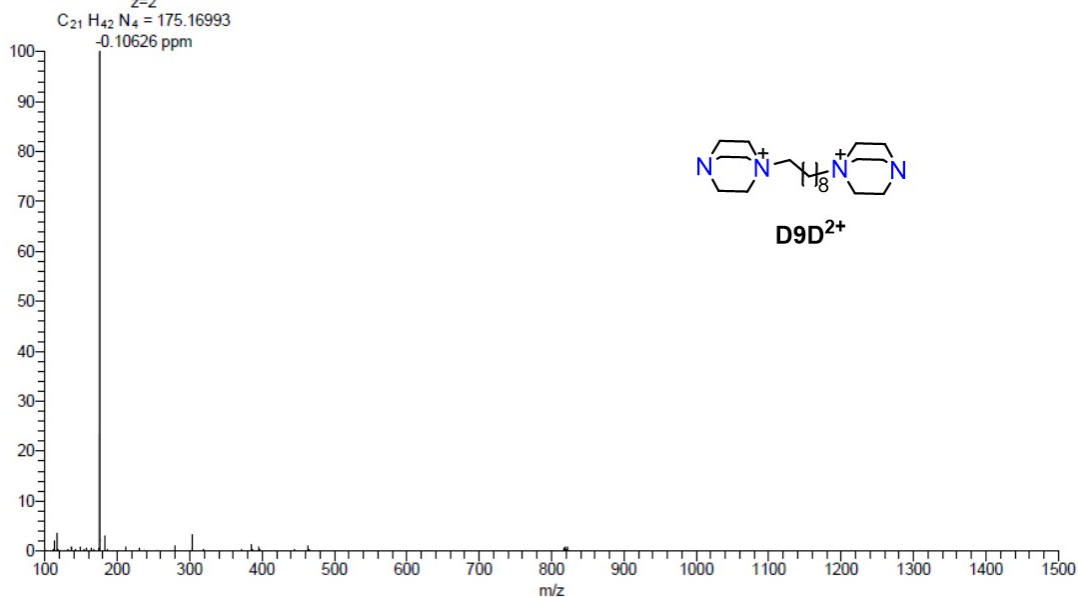
^1H NMR spectrum (500 MHz, CD_2Cl_2 , 298 K) of compound **D9D-2BArF**



^{13}C NMR spectrum (125 MHz, CD_2Cl_2 , 298 K) of compound **D9D-2BArF**

Positive mode

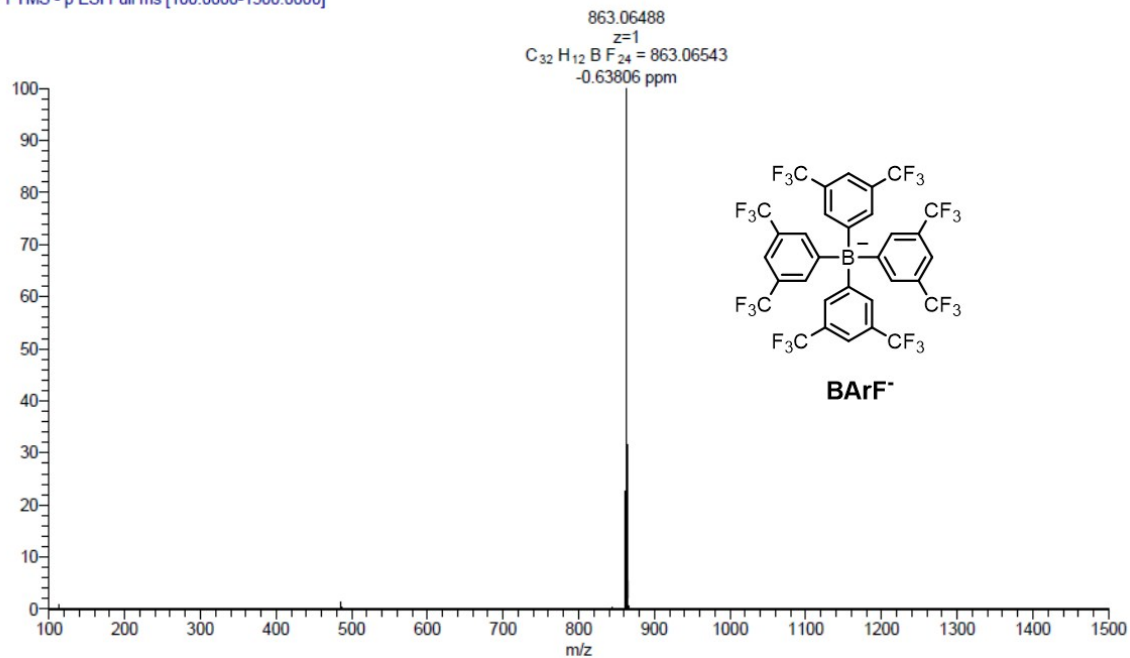
D9 #13 RT: 0.14 AV: 1 NL: 8.66E8
T: FTMS + p ESI Full ms [100.0000-1500.0000]
175.16991
z=2



ESI mass spectrum (positive mode) of compound **D9D-2BArF**

Negative mode

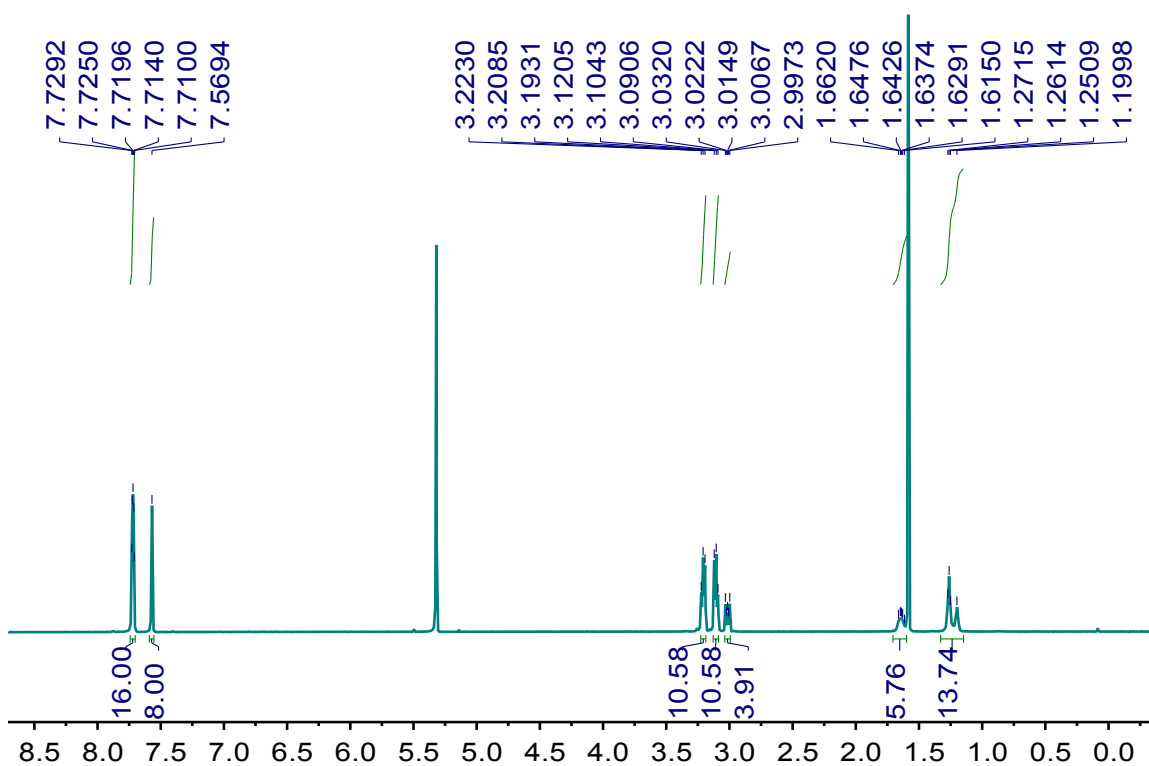
D9 #10 RT: 0.11 AV: 1 NL: 4.72E8
T: FTMS - p ESI Full ms [100.0000-1500.0000]

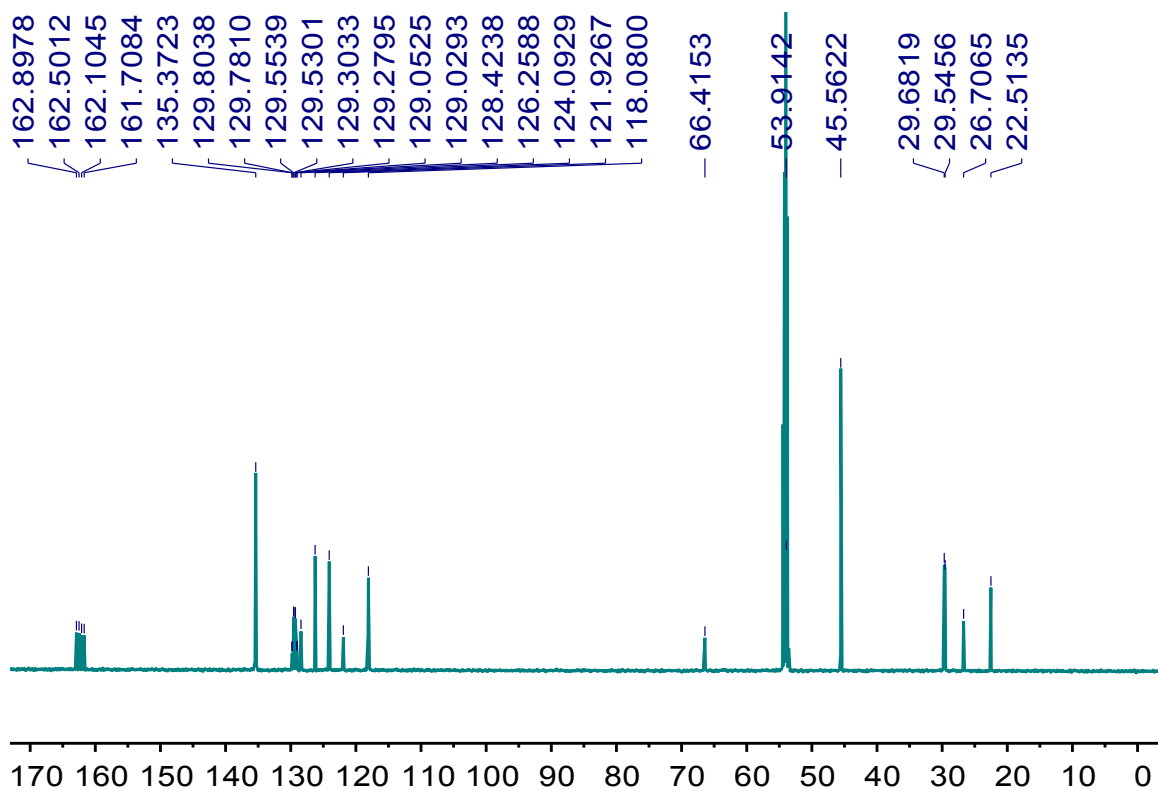


ESI mass spectrum (negative mode) of compound **D9D-2BArF**

D10D-2BArF: It was prepared from its bromide salt by using the same procedure as that for **D9D-2BArF**; **D10D-2BArF** was obtained as a white solid (0.50 g, 96 %).

m.p. 149-150 °C; ^1H NMR (500 MHz, CD_2Cl_2 , 298 K) δ [ppm] = 7.73 - 7.71 (m, 16H), 7.57 (s, 8H), 3.21 (t, $J = 7.4$ Hz, 10H), 3.11 (t, $J = 7.5$ Hz, 10H), 3.04 - 2.99 (m, 4H), 1.66 - 1.62 (m, 6H), 1.33 - 1.15 (m, 14H); ^{13}C NMR (125 MHz, CD_2Cl_2 , 298 K): δ [ppm] = 162.3 (q, $^1J_{\text{CB}} = 50$ Hz), 135.4, 129.4 (q, $^2J_{\text{CF}} = 50$ Hz), 125.2 (q, $^1J_{\text{CF}} = 270$ Hz), 118.1, 66.4, 53.9, 45.6, 29.7, 29.6, 26.7, 22.5; HRMS (ESI): m/z calcd for $[\text{M}-2\text{BArF}]^{2+}$ $\text{C}_{22}\text{H}_{44}\text{N}_4^{2+}$, 182.1778; found 182.1777 (error = -0.1 ppm); calcd for $[\text{BArF}]^-$ $\text{C}_{32}\text{H}_{12}\text{BF}_{24}^-$, 863.0654; found 863.0652 (error = -0.3 ppm).

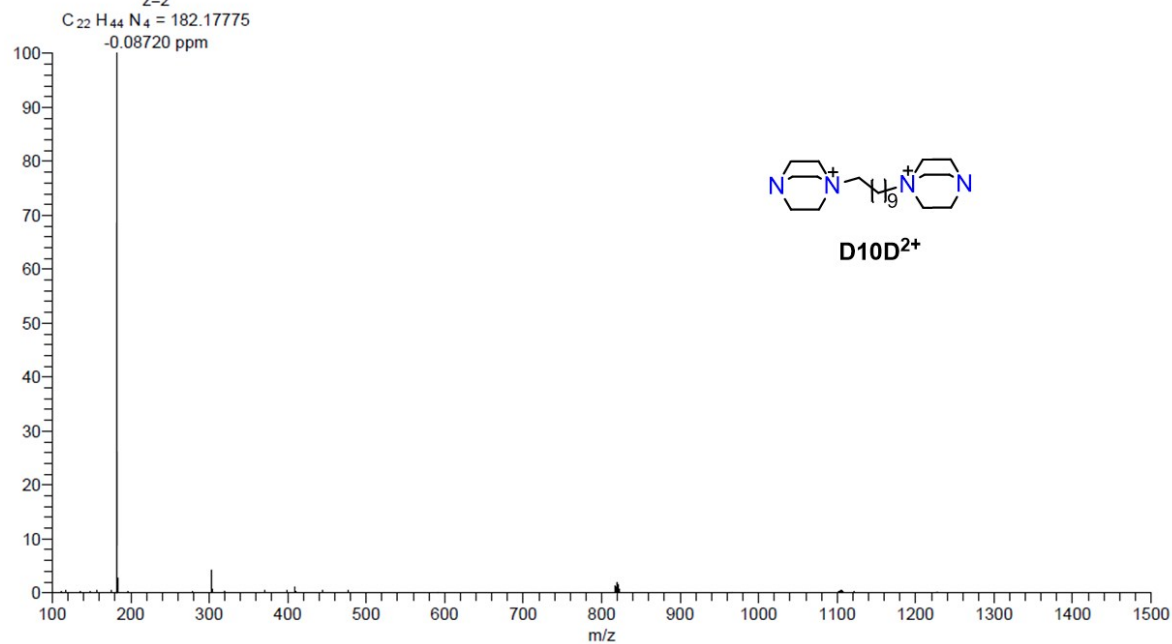




^{13}C NMR spectrum (125 MHz, CD_2Cl_2 , 298 K) of compound **D10D-2BArF**

Positive mode

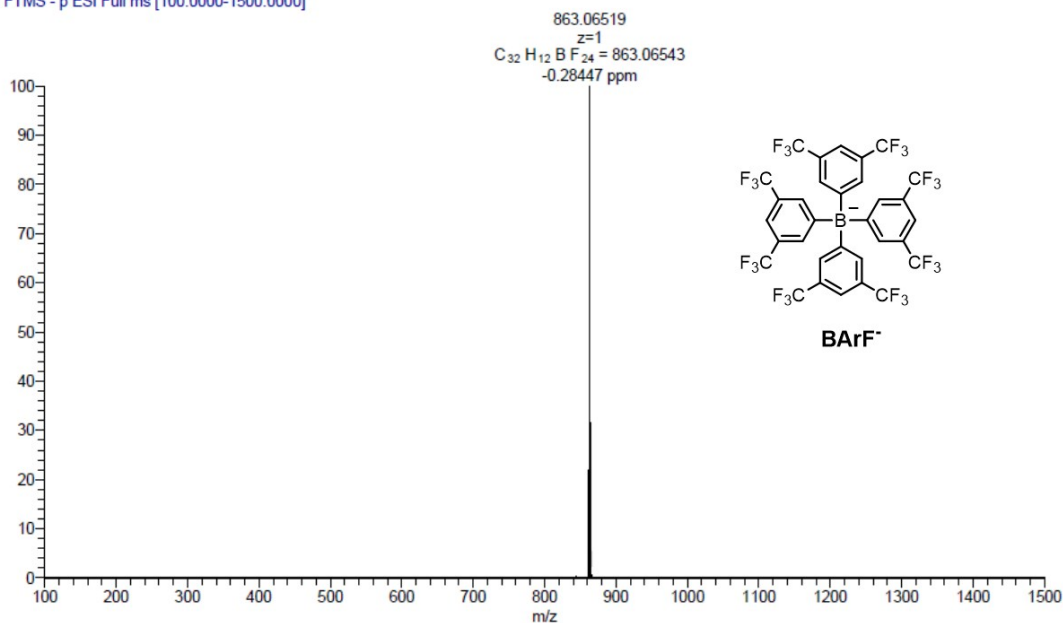
D10 #11 RT: 0.12 AV: 1 NL: 3.29E9
T: FTMS + p ESI Full ms [100.0000-1500.0000]
182.17773
z=2



ESI mass spectrum (positive mode) of compound **D10D-2BArF**

Negative mode

D10#10 RT: 0.11 AV: 1 NL: 1.08E9
T: FTMS - p ESI Full ms [100.0000-1500.0000]



ESI mass spectrum (negative mode) of compound **D10D-2BArF**

5. References.

- [1] *CrysAlisPro* (Version 1.171.38.41.), Rigaku Oxford Diffraction, 2015.
- [2] R. C. Clark, J. S. Reid, *Acta Crystallogr., Sect. A: Found. Crystallogr.*, 1995, **51**, 887-897.
- [3] G. M. Sheldrick, *Acta Crystallogr., Sect. A: Found. Adv.*, 2015, **71**, 3-8.
- [4] G. M. Sheldrick, *Acta Crystallogr., Sect. C: Struct. Chem.*, 2015, **71**, 3-8.
- [5] Z. He, G. Ye, and W. Jiang, *Chem. Eur. J.*, 2015, **21**, 3005-3012.
- [6] F. Jia, Z. He, L.-P. Yang, Z.-S. Pan, M. Yi, R.-W. Jiang, and W. Jiang, *Chem Sci.*, 2015, **6**, 6731-6738.
- [7] Y.-L. Ma, H. Ke, A. Valkonen, K. Rissanen, and W. Jiang, *Angew. Chem. Int. Ed.*, 2018, **57**, 709-713.
- [8] G. B. Huang, S. H. Wang, H. Ke, L. P. Yang and W. Jiang, *J. Am. Chem. Soc.*, 2016, **138**, 14550-14553.
- [9] C. Li; X. Shu, J. Li, J. Fan, Z. Chen, L. Weng and X. Jia, *Org. Lett.*, 2012, **14**, 4126-4129.